AESB3400 Bachelor Thesis

# Measuring gamma radiation with a portable gamma ray spectrometer at a measuring location consisting of multiple rock types.

Tim Meijer, 4473825

Supervisors:

Adriana Guatame-Garcia
&
Dominique Ngan-Tillard

# Contents

## Abstract

A pilot research was set up to determine the possibilities for using gamma-ray spectrometry to find possible value in mine waste piles. These waste piles consist of different waste rocks without any value and ore that was processed incorrectly. This method, if proven effective, will be used on mine waste from different commodities all over the world. However, there will be started with the waste pile Halde Haniel in the Ruhr area in Germany. The Ruhr area has been selected because of the manageable travelling time from Delft, the long history of coal mining activities in the area and the open-access of the waste pile. The thriving days of coal mining have left us with large amounts of waste piles (170 waste piles in the Ruhr area). Therefore, it will be essential to know if these waste piles have an impact on the environment by emitting gamma radiation. In Europe, this problem has not been addressed. However, in other countries, these waste piles are the cause of increased health risks. The Halde Haniel waste pile is a human-made object and consist mainly of shale, sandstone and bits of coal. Gamma-ray spectrometry is often used to determine lithology of a rock formation. To determine the lithology measurements are done on outcrops present in nature. In most literature gamma-ray spectrometry is used to determine the lithology of rock formations. However, in this research, the measuring location is a human-made object, which has destroyed the natural sequencing of the rocks. Therefore, the measurements taken on the Halde Haniel makes the research more challenging.

Therefore, the accuracy of the measurements done on a site consisting of multiple rocks, such as the Halde Haniel, are essential to know in order to apply this method in future research. Field measurements were taken for two different reasons. First, a control study was executed in the Green Village in Delft. The main goal of these measurements was to select a correct measuring time for the measurements at the Halde Haniel waste pile. The rest of the measurements were done at the Halde Haniel waste pile. At the Halde Haniel waste pile, four different measuring locations were selected. From the results can be concluded that the amount of gamma radiation emitted from the Halde Haniel waste pile is higher than at a location without mining activities. However, this increase is still not high enough to result in health risks. The measuring error could not be determined to a satisfactory standard, because of the lack of soil moisture samples and the significant impact of soil moisture on the error of measurements. Gamma-ray spectrometry should be supported with information about the lithology and the chemical composition of the rocks, because otherwise finding value in waste piles will be hard.

# 1 Introduction

## 1.1 Introduction

The thriving days of coal mining in Europe are left in the past. However, the vast amount of spoils are still a reminder of the once flourishing industry. The annual global production of spoil in 2009 is estimated to be 22240 million tons from coal mining and 3900 million tons from lignite mining (Doka, 2009). A large amount of this spoil will be put in large waste piles on the surface. In 2018 the last underground hard coal mine closed its doors. However, the closed mines must not harm the environment. Even years after all the mines have been closed.

The effect of these waste piles on the environment has not been addressed in Europe. Nevertheless, in other regions, waste piles are having a substantial negative impact on the environment by emitting gamma radiation. The effects on the environment of two waste dumps from different mines, the Tudor Shaft gold mine in South Africa (Njinga and Tshivhase, 2016) and the Maiganga coal mine in Northeast Nigeria (Kolo et al., 2017), have both resulted into excess lifetime cancer risk for the people living in the area.

This pilot research was set up to determine the possibilities for using gamma-ray spectrometry to find possible value in waste piles from mines. These waste piles consist of different waste rocks without any value and ore that was processed incorrectly. This method, if proven effective, will be used on mine waste from commodities all over the world. However, there will be started with a waste pile in the Ruhr area in Germany. The Ruhr area has been selected on the manageable travelling time from Delft. Also, the Ruhr area has seen coal mining activities during the past 200 years. The development of waste piles has been going for the same period. The Halde Haniel waste pile will be used as the research area for this study. The Halde Haniel waste pile is one of the 170 waste piles present in the Ruhr area (Harnischmacher, 2007). The Halde Haniel waste pile is one of the biggest waste piles in the Ruhr area with a height of 180 meters and an area of 110 hectares(Hellman, 2020) and the only one open to the public (with this size).

An efficient measuring method will have to be developed to measure the amount of the radiation emitted from these waste piles. A portable gamma-ray spectrometer has been used before to map different geological formations (Myers, 1987, Løvborg, 1984 and Parkinson, 1996). These formations mainly consisted of one type of rock, and this technique gives similar results to borehole log measurements. However, in this research, the measuring location is a human-made object, which has destroyed the natural sequencing of the rocks. Therefore, the measurements taken on the Halde Haniel makes the research more challenging.

## 1.2 Objective

The objective is to test whether the gamma-ray spectrometer can be used at multiple rock formation sites, such as the Halde Haniel waste pile. To prove this method works, the reliability of the measurements done by a portable gamma-ray spectrometer on the Halde Haniel waste pile will be determined.

This objective has resulted in the following three research questions and hypothesis: first, is the measured radiation at the Halde Haniel site a hazard for the environment or humans? The amount of radiation is expected to be higher at the Halde Haniel waste pile, than the gamma radiation emitted from soils where no mining activity has taken place. Secondly, is there a spatial difference in the waste pile Halde Haniel? Spatial differences are expected, because the mine progresses through a difference in lithology as the mine progresses through time. Also, not all the waste has been dumped on the site at the same moment. How accurate are the measurements that are done with the portable gamma-ray spectrometer? There will be assumed that accuracy will depend on the precision of the measuring device and the measuring error of the portable gamma-ray spectrometer.

## 1.3 Outline of the thesis

In chapter 2, there will be started with a literature study on the study area, which is the Ruhr area in Germany. Here the emphasis will put on the coal mining in the Ruhr area and also the development of waste piles because of the mining activity. In chapter 3, gamma-ray spectrometry will be explained in more detail. Here an in-depth literature study is done on how the measuring device works, from which rocks the radiation comes from and what the hazard for humans will be. In chapter 4, the methods used during the fieldwork of this study will be explained. In chapter 5, the measurements during this research will be divided into two parts. First of all, some measurements were done in Delft to determine the measuring time. Five different measuring times (1, 2, 3, 4 and 6 minutes) were tested on varying soil types. The measurements at the waste pile Halde Haniel were done in four different measuring patterns. These measuring patterns were grouped on the similarity of the measuring location. The measuring patterns were chosen in such a way that a large part of the Halde Haniel waste pile could be mapped in the time available. The measuring patterns are as follows: random, a straight line, on the slopes of the waste pile Halde Haniel and a square of measurements. These results are elaborated on in the discussion, and the report ends with the conclusion.

# 2 The study area

In this section, some general information about the study area is explained. Also, the mining activities and the local geology will be touched on. In the last part, more clarity will be given on the measuring location Halde Haniel.

## 2.1 The Ruhr area

The Ruhr area is located in the western part of Germany (see figure 1). The Ruhr area is a metropolitan area with an overall population of 5.7 million people living in 11 cities with more than 100 000 inhabitants and four districts (Harnischmacher, 2007). This area has seen significant development throughout recent history. This development has been the result of the favourable geology.

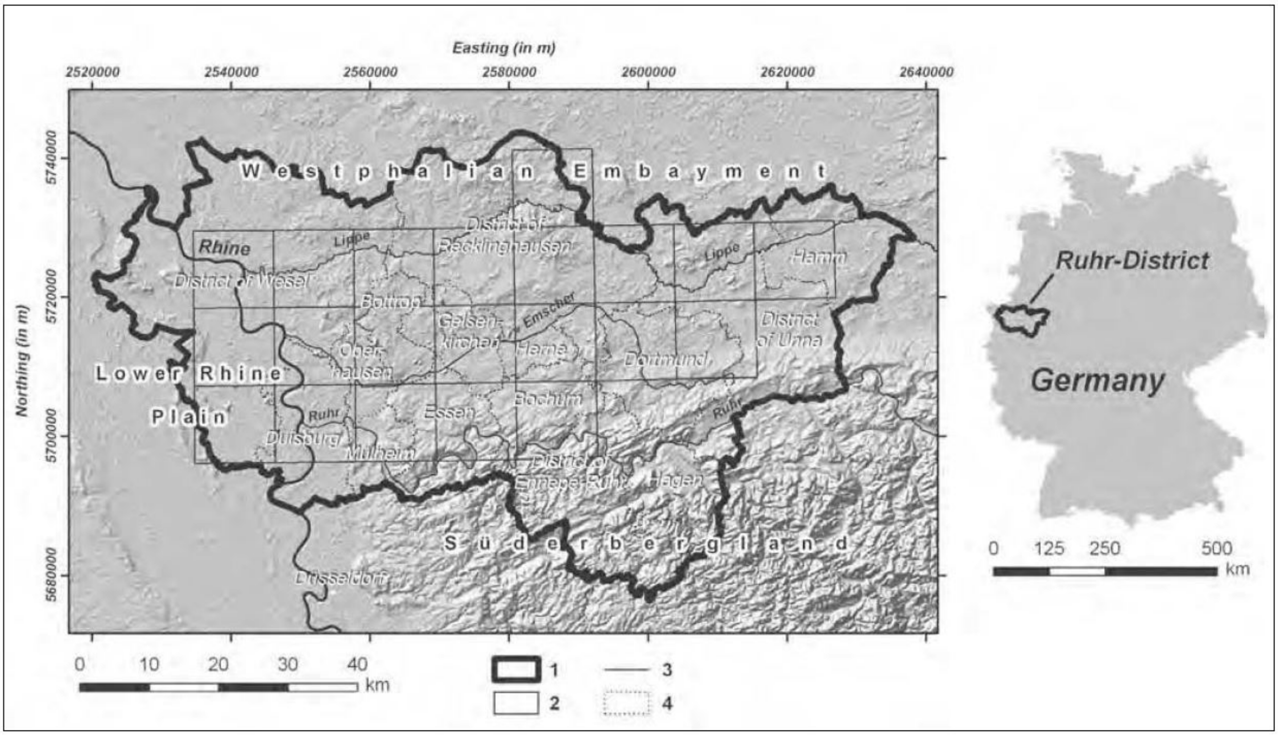


**Figure 1:** A map of the Ruhr area with to the right of it an overview of Germany with the Ruhr area highlighted (Harnischmacher, 2010)

### 2.1.1 Coal mining in the Ruhr area

Hard coal has been mined for over 200 years ago in the Ruhr district (Frank, 2009). Since 200 years ago no machines were available for the coal mining, so all the mining activities started at the surface. The Upper Carboniferous coal-bearing strata are exposed on the surface along the Ruhr valley (Harnischmacher, 2007). In the cross-section, shown in figure 2, the southern area near the Ruhr river, the coal seams are located on the surface. After the introduction of more heavy machinery, the mining area expanded more towards the north.

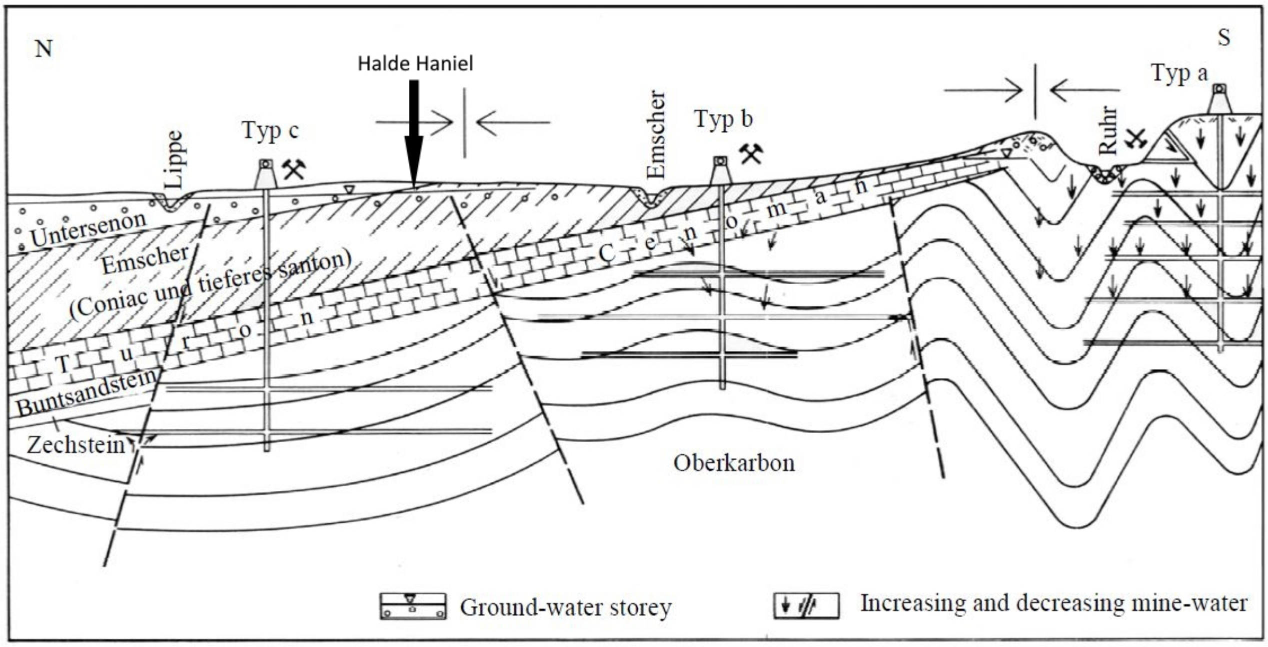


**Figure 2:** A schematic cross section of the Ruhr area with the important formations highlighted and the orientation is from North to South (Frank, 2009). Added to the figure is the approximate location of the Halde Haniel waste pile.

The use of machines resulted that the Ruhr area was one of the biggest producers of coal for the European market throughout the late 19th, 20th and beginning of the 21st century. The favourable geology of the region and the way the coal-bearing layers were deposited have been vital in the development of the Ruhr area. The Ruhr area had vastest coal reserves in Europe, the seams being, relatively, both thick and numerous (Harris, 1946). So besides the geology, the location is also ideal for the massive exploration of these coal fields. To excess the deeper the coal-bearing layers, shafts had to be sunk at various locations. The sinking of shafts resulted in big waste dumps of a variable composition. In the north, west, and east the coal-bearing strata lie under more recent deposits of shale, limestone, sandstone, and chalk (Harris, 1946). These deposits will be explained in more detail in the next paragraph.

### 2.1.2 Geology of the Ruhr area

The geology of the Ruhr area was formed by geological processes that took millions of years (Nordrhein-Westfalen, 2015). All the coal-bearing layers were developed during the Carboniferous. However, a start will be made one period earlier, in the Devonian (from 420 until 360 million years ago). During the Devonian, the deposition consisted of hundreds of meters of clay, silt, and sandstone. Also, thick limestones were formed, that represent the extensive Devonian reefs present in the warm tropical sea. During the Carboniferous (from 360 until 300 million years ago) thick coal layers were formed. Vast coastal plains dominated this period with swamps and dense forests stretching to the north of Germany. The following three periods, Permian and, Triassic and Jurassic (from 300 until 145 million years ago), the deposition of rocks was minimal. However, in the Cretaceous (from 145 until 66 million years ago), a lot of different rocks were deposited in the Ruhr area. These rocks mainly consisted of sediments left by the sea such as sand, limestone, and clay marl. In the Tertiary again, the deposition in the Ruhr area was minimal. In the most recent history of the Quaternary (from 66 until 23 million years ago) mainly deposited sand and gravel terraces of the rivers, moraine of the glaciers and some sandy and silty wind deposits (Nordrhein-Westfalen, 2015). During this study, the focus will be on the following rock types: siltstone, sandstone, claystone, and limestone from the Devonian and, coal from the Carboniferous and, sandstone, limestone and clay marl from the Cretaceous and, sand/gravel deposits, moraine of glaciers and sandy, silty wind deposits from the Quaternary.

## 2.2 Measuring location Halde Haniel

The fieldwork for this study will be conducted on one of the many coal mining waste piles present in the Ruhr area. The Halde Haniel waste pile is located between Bottrop and Oberhausen (see figure 3). The Halde Haniel waste pile is one of the 170 waste piles present in the Ruhr area (Harnischmacher, 2007). The Halde Haniel waste pile is one of the most massive waste piles in the Ruhr area with a height of 180 meters and an area of 110 hectares(Hellman, 2020) and the only one open to the public (with this size). All the material came from the neighbouring mines Prosper-Haniel I and II. The location of Halde Haniel and the mines is shown with black arrow in figure 2.


**Figure 3:** The location of the Halde Haniel with two large cities as Bottrop and Oberhausen surrounding the waste pile (Hellman, 2020)

The first waste piles were deposited as soon as mining started in the area. The first waste piles mainly consisted of cone shape heaps with steep slopes (Harnischmacher, 2007). These new waste piles were represented as the first generation (see figure 4). These cone-shaped dumps created different hazards for humans. The two most important risks were spontaneous combustion and landslides (Gawor et al., 2011).

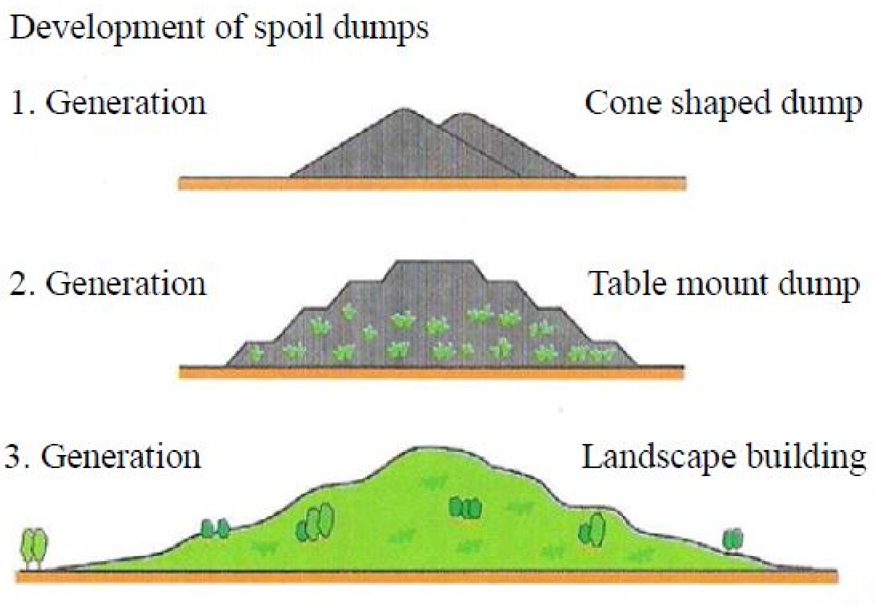


**Figure 4:** Three generations of waste pile construction. Were the first generation consisted of a cone shaped dump with steep slopes. The second generation with more steps in the slopes. At last the third generation were the focus was on the integration with the existing landscape. (Frank, 2009)

The waste piles were redesigned in a better way so that landslides will be prevented. The redesign of these waste piles leads to the development of the second generation of waste piles (see figure 4). The second-generation waste piles are shaped with different steps and a flat peak. The second-generation waste piles saw a reduction in the number of landslides, but the design was not flowing well with naturally acquiring terrain (Harnischmacher, 2007). The improving mining techniques reduced the spontaneous combustion of the waste piles.

In the 1980s, strict laws were made by the German government to improve the structural and ecological requirements (Harnischmacher, 2007). These laws resulted in waste piles that merged better with the existing landscape (see figure 4). With the third generation, more emphasis was put for future usage. Different waste piles (such as the Halde Haniel) were made attractive for recreation use.

At the Halde Haniel waste pile multiple recreational walking and mountain biking tracks are present. The walking trail has a collection of both religious and industrial art pieces along the trail. When arriving at the summit, there is a location for religious celebrations and also a small amphitheatre that can host a variety of events (Hellman, 2020).

# 3 Gamma ray spectrometry

In this section, the basics of gamma-ray spectrometry will be explained with an emphasis on the origin of gamma rays, the measuring device, the placement of the measuring device, the measuring time and the precision of the measurement. After this, the environmental effects influencing the measurements will be discussed. Lastly, the radiation of different rocks will be shown and the hazards for humans.

## 3.1 The origin of Gamma-Rays

The world is always looking for stability, and this is especially the case with an unstable nucleus. Radioactive decay of an unstable nucleus will happen to achieve stability. In attaining stability, a radioactive nucleus will emit alpha particles, beta particles or gamma rays, depending on the neutron to proton ratio in the unstable nucleus (Myers, 1987). An example of such a decay series can be found in figure 5. Although at least twenty naturally occurring elements are known to be radioactive, only Uranium, Thorium and an isotope of Potassium are of importance in most geological exploration (Myers, 1987). All the other elements do not emit enough radiation or are rarely found in nature. Therefore, the gamma-ray measuring devices will only be measuring Uranium, Thorium and Potassium.

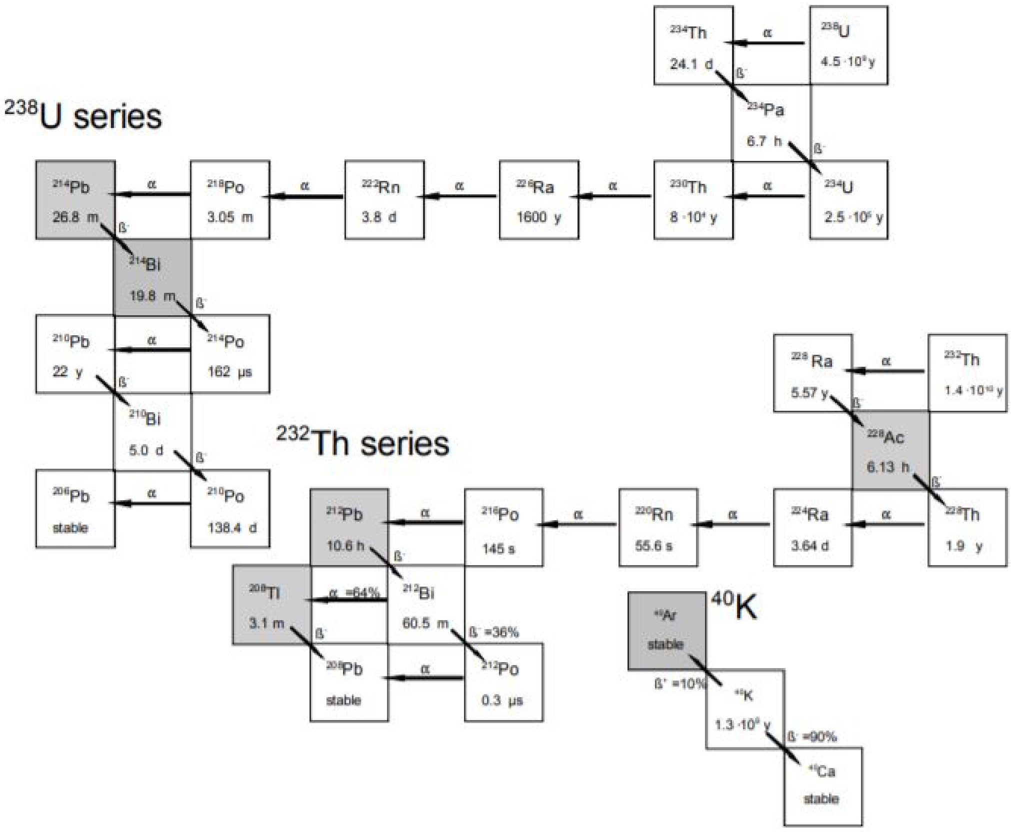


**Figure 5:** Simplified decay schemes of $^{238}$U, $^{232}$Th, and $^{40}$K with life-time in years (y), months(m), days (d), hours (h) and seconds (s). The most relevant gamma-ray emitters are marked by the grey boxes (Koomans, 2000)

Different techniques are used to determine the amount of radiation emitted per element. For Potassium, a fixed proportion of $^{40}$K occurs in the natural environment. These gamma rays can be used to estimate the total amount of K present (IAEA, 2003). Since $^{40}$K occurs in nature as a fixed ratio to other non-radioactive, isotopes of Potassium. Thus, the estimation of K is direct, and results are reported in % K (per cent Potassium). While for Uranium and Thorium the gamma radiation is not directly emitted from the natural radioisotopes, expect these elements will decay in series that terminate into a stable isotope. During this decay series, the different radioactive daughter products are used to estimate their concentrations (see figure 5). Therefore, the estimation of U and Th by gamma-ray spectrometry is thus indirect, and the results are reported in ppm eU or eTh (parts per million of equivalent uranium or Thorium) (IAEA, 2003).

For the quantification the different amounts of ionizing radiation, select units are used to reduce the chance of mistakes. The SI unit of radioactivity is designated to be becquerel (Bq in $s^{-1}$) rather than the reciprocal second, and the SI units of absorbed dose and dose equivalent are designated to be Gray (Gy) and Sievert (Sv), respectively, rather than the joule per kilogram (J/kg) (ISU, 2006). In this study, a variation of Gray will be used. When measuring with the GS-512i Geostatics, all the data is given in nano Gray per hour (nGy/h). Therefore all the information in other units will be converted into nano Gray per hour (nGy/h).

### 3.2 The measuring device

During this study, all the measurement are done with the SatisGeo GS-512i. This device has a detection probe that contains sodium iodide activated with thallium NaI(TI) scintillation detector. The device is calibrated using a reference radiation source, typically Caesium $^{137}$Cs, which is mounted at the base of the probe (SatisGeo, 2020). NaI(TI) is commonly used as a scintillation Phosphor. The use as a scintillation detector is because NaI(TI) has a high atomic number, which results in good stopping power for the gamma radiation. Furthermore, NaI(TI) has a high luminescent efficiency, which results in considerable pulse heights for low energy gamma-ray interactions (Myers, 1987).

There are different types of gamma-ray detectors on the market, but the scintillation and semiconductor-based detectors are the most common to use. The scintillation detector uses light to determine the amount of energy emitted, while the semiconductor-based detector is depending on the detection of charge carriers. Both of these detectors can determine the amount of energy and the number of existing particles. The resolution of the semiconductor-based detectors is better than the scintillation detector. However, the semiconductor-based detector is cooled using by liquid nitrogen. So, for field use, these semiconductor-based detectors are not suitable (Knoll, 2012).

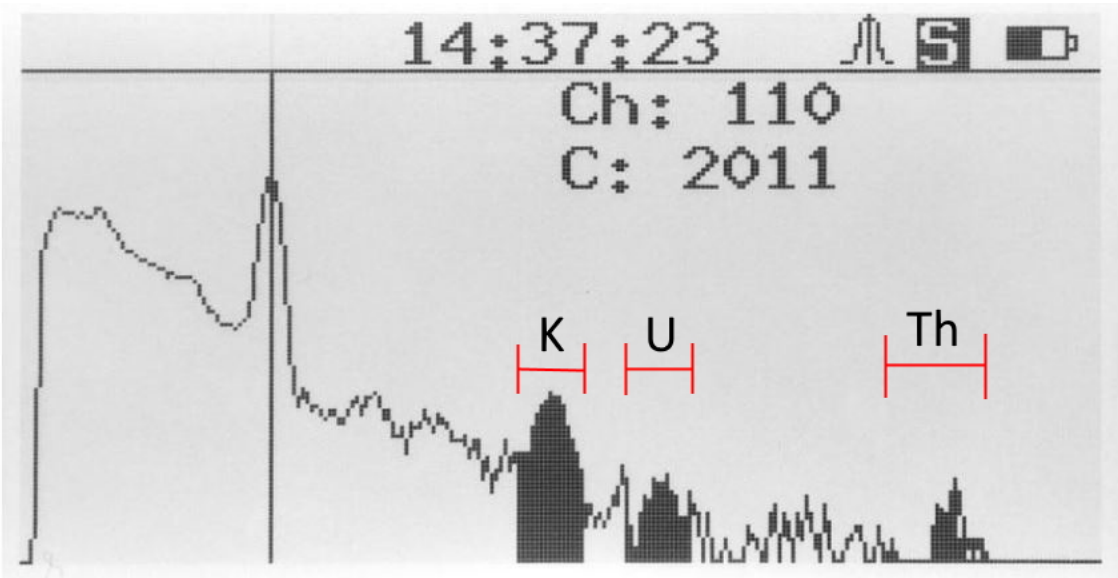


**Figure 6:** A spectrum graph with on the vertical axis the amount of count and on the horizontal axis the specific channel and the range of the K, U and Th indicated (SatisGeo, 2020)

The GS-512i gives, besides the data in a table, also a spectrum graph with information. An example of the spectrum graph plotted by the GS-512i is shown in figure 6. These spectrum graphs are updated continuously during the measuring period. Each channel is specific for a certain element. The reference peak is set on channel 110.0, provided a $^{137}$Cs 662 keV energy line is used for automatic spectrum stabilization (SatisGeo, 2020). When the device does this stabilization, the energy calibration will start. The energy calibration will be 6 keV/channel (SatisGeo, 2020). The ROI (Region Of Interest) is the energy window for a specific element. These specific energy windows are fixed for Potassium, Uranium and Thorium. ROI2 indicates channel limits and registered counts in the Potassium (K) energy window, covering the $^{40}$K 1461 keV gamma energy line (33 channels) (SatisGeo, 2020). The channel range for $^{40}$K is from channel 220 until channel 252. ROI3 indicates channel limits and registered counts in the uranium (U) energy window, covering the $^{238}$U 1764 keV gamma energy line (33 channels). The channel range for $^{238}$U is from channel 268 until channel 300. ROI4 indicates channel limits and registered counts in the Thorium (Th) energy window, covering the $^{232}$Th 2615 keV gamma energy line (67 channels). The channel range for $^{232}$Th is from channel 387 until channel 453 (SatisGeo, 2020).

### 3.3 Placement of the measuring device

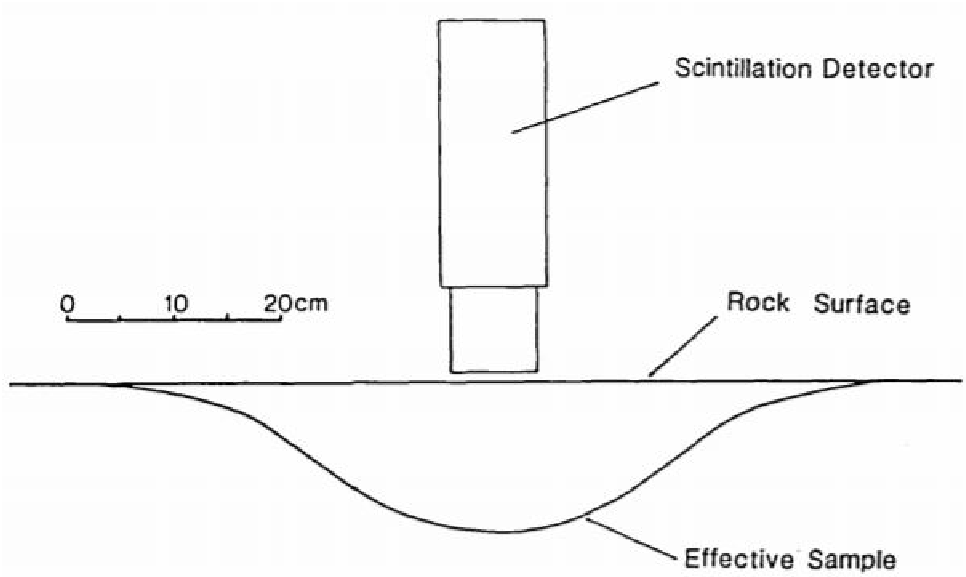


**Figure 7:** Sampling size of the portable gamma spectrometer (Myers, 1987). With a size of approximately 1 m in diameter and 15 cm deep (Parkinson, 1996)

In figure 7, there is shown how the portable gamma-ray spectrometer will take a sample. The device samples in a bowl-shaped region (Løvborg, 1984). The sampling size is approximately 1 m in diameter and 15 cm deep (Parkinson, 1996), which is a volume of 0,16 $m^3$. The way the spectrometer is placed on the surface has a great effect on the sampling size of the portable gamma-ray spectrometer. Throughout this study, the measurements should be as consistent as possible. Therefore, possible variations in the placement of the measuring device should be avoided or kept to a minimum. These variations in placement are shown in figure 8, wherein figure 8a will measure less rock, which will result in a decrease in the amount of gamma radiation recorded when comparing it to a flat measuring location. While in figure 8b, the device will measure more rock, which will lead to an increase in the amount of radiation recorded when compared to a flat measuring location.

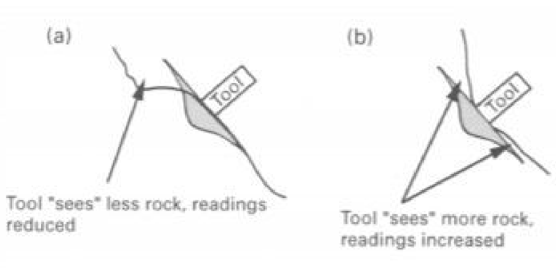


**Figure 8:** The effect of placement on the sampling size. Where figure (a) will see less rock, which will result in decrease in the amount of gamma radiation measured and figure (b) will see more rock, which will result increase in the amount of gamma radiation (Parkinson, 1996)

Differences in the measurement placement will be kept to a minimum. Since, the measuring area consists of a flat surface or a flat surface with an angle. The other more rough measuring locations will be avoided to make the measurements more consistent.

### 3.4 Measuring time

In theory, the GS-512i of SatisGeo could measure for an extremely long time. However, this will not be practical for a field survey. The practical limit of the counting time in the field is 10 minutes (Myers, 1987). The GS-512i depends on emission of enough gamma-ray energy to determine all the elements accurately. This energy limit will be achieved at different times, depending on how radioactive the rocks will be. Therefore, A possibility will be that the amount of energy emitted by the rocks is below the detection limit, if this would be the case then gamma-ray spectrometry is not a suitable technique (Myers, 1987). Two factors will determine the duration of the field measurements. These factors consist of a trade-off between the energy intensity and the length of the measurement. The local geology consists of varying rock types with different ideal measuring time. For the more radioactive rocks such as shales 2-4 minutes is enough and, for sandstones the measuring time will increase to 4-6 minutes and for limestone, the limit of 10 minutes will be approached (Myers, 1987).

### 3.5 The precision and accuracy of the measurement

The difference between precision and accuracy should be explained before continuing with this section. Precision is a measure of statistical significance, while accuracy is used for expressing the effect of calibration errors (Løvborg, 1984). A precision of about 0.1 % K, 0.4 ppm eU and 0.6 ppm eTh (or 1.31 [nGy/h] K, 2.27 [nGy/h] U and 1.5 [nGy/h] Th) can be expected from field assays with a scintillation gamma-ray spectrometer using a sampling time of 4 minutes (IAEA, 2003). However, looking at the accuracy of the measurements, the errors will become larger. As stated by Parkinson (1996) the accuracies will be $\pm 7\%$ for K, $\pm 15\%$ for Th and $\pm 30\%$ for U.

### 3.6 Environmental effects

Several environmental effects will have a significant impact on the ground measurements. First of all, the vegetation cover of the measuring area, which should be kept to a minimum. Secondly, the measurements should be done on a day with dry soil conditions if possible. Lastly, the effects of weathering should be taken into account.

Vegetation can negatively affect the measurements. The main reason for this is because vegetation is non-radioactive. For example, just 2 cm of vegetation cover can reduce the radiation penetrating to the ground surface by 35 per cent (IAEA, 2003). With this in mind, it is crucial to make sure that on the measuring area, no vegetation is present. Since, all the measuring locations will be selected on the absence of vegetation. The adverse effects of vegetation cover will be kept to a minimum. Therefore, vegetation will not influence the current research, but maybe relevant in the future.

The water content in the soil harms the measurement. Soil moisture can be a significant source of error in gamma-ray surveying. Ten % of soil moisture will give an accuracy error of approximately ten % (IAEA, 2003). With this knowledge, there should be a soil sample be taken to approximate the moisture content in the soil. If taking samples is not possible, then the human senses should be used to estimate the soil moisture percentage.

Weathering of rocks is a naturally acquiring geological process, which will show effects in the amount of gamma radiation that is emitted. Since the study area only consists of sedimentary rocks, the effects of the weathering will be reduced. Little U and Th occurs in leachable form, since sedimentary rocks have been through at least one weathering cycle already (Myers, 1987). Even though the leachable amount of U and Th are small, the effects of weathering should still be taken into consideration. The effect of weathering is especially the case on slopes were rocks move because of gravity. On the flat surface, weathering through natural processes will have a more significant impact. These natural processes are mainly rain, snow, wind and sunlight.

### 3.7 Gamma radiation from different rocks

The average recorded amount of radiation and the standard deviation from the different rocks that are present in the Ruhr area are shown in the appendix I in table A1. The information in table A1 was taken from Myers (1987), David G. Coles and Ondov (1979), Bem et al. (2002), Tracy and Prantl (1985), Fardy et al. (1989) and Beck (1989). The information about the different rocks will help to determine where the radiation is coming from. Looking at figure 9, the error of the measurements is high; this is the results of the variation in deposition and composition of the different rock types. The composition of sandstone is completely different when comparing it to a shale. Therefore, figure 9 will indicate which type of rock the radiation is coming from. The data from figure 9 can be clustered into two groups. The first group consisting of shale and sandstone. The amounts of radiation from K, U, and Th are in the same range for these rock types. The other group consist of coal and limestone where coal and limestone both emit approximately the same amounts of radiation from K, U, and Th.

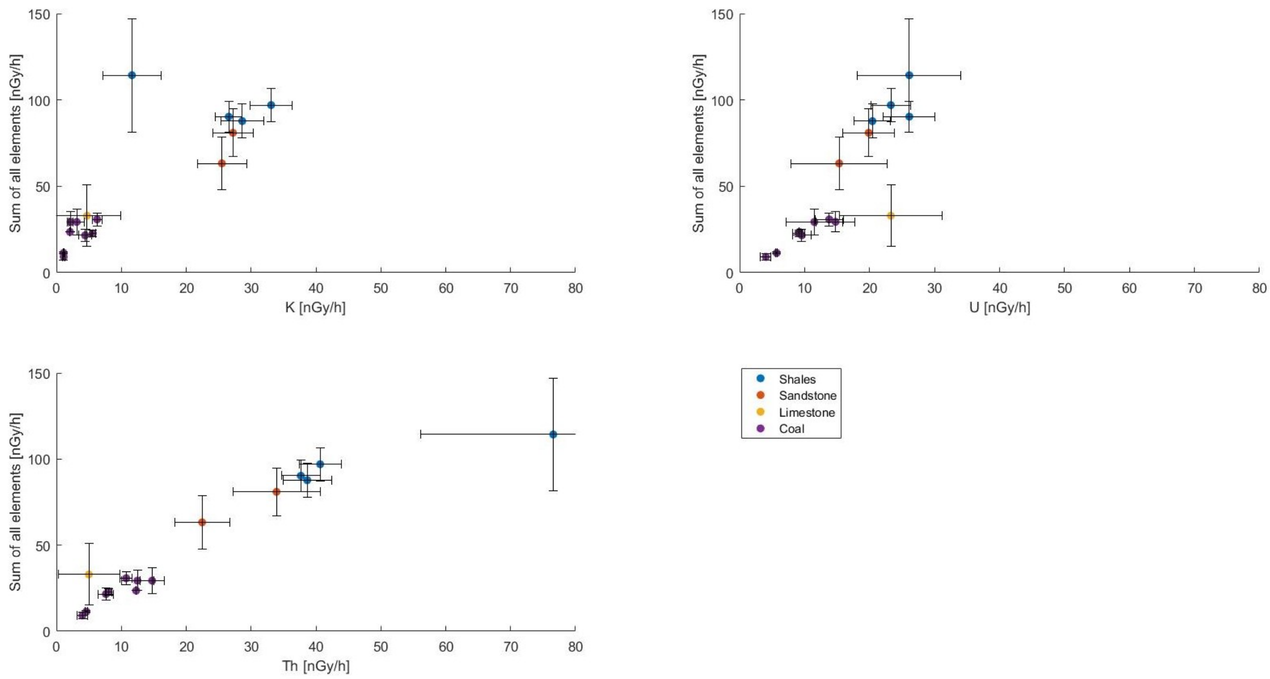


**Figure 9:** The amount and standard deviation of gamma radiation emitted by K, U, Th from different rock types. The information in this figure was taken from Myers (1987), David G. Coles and Ondov (1979), Bem et al. (2002), Tracy and Prantl (1985), Fardy et al. (1989) and Beck (1989)

### 3.8 Hazard for humans (Maximum allowed level of radiation without resulting in adverse effects for humans)

There are a lot of different ways of measuring the amount of radiation a person can be exposed to. Natural and background radiation is continuously emitted from the earth. However, there is a maximum on the amount of radiation people can be exposed.

The absorbed gamma dose rate, D ($nGyh^{-1}$) consists of an uniform distribution of K, Th and U (Habib et al., 2018 and UNSCEAR, 2000). The annual effective dose rate, E ($mSvyear^{-1}$), represents the amount radiation in air, that a person will received. These formulas are on the basis of UNSCEAR (2000) (Eq. (1)):

$$E = D * 10^{-3} * 1.23 \tag{1}$$

The excess lifetime cancer risk, ELCR ($Sv^{-1}$), caused by the annual effective dose due to external exposure was estimated using expression (2) (IRCP, 1990):

$$ELCR = E * ALT * RF \tag{2}$$

Where ALT is the average lifetime (80 years for German people) and RF is the risk factor based on the fatal cancer risk per Sievert and stochastic effects (Habib et al., 2018). The IRCP (1990) uses a value of $0.5 * 10^{-4}$ for the public exposure . According UNSCEAR (2000) the excess lifetime cancer risk should not be higher than $4 * 10^{-2} Sv^{-1}$. If this value is exceeded, then the radiation will be considered a hazard.

# 4 Methods

In the next chapter, all the different methods that were used during this research are explained.

For all the measurements, the same measuring device has been used: The portable gamma-ray spectrometer GS-521i developed by SatisGeo. After all the measurements were done in the field, the data interpretation was made using MATLAB. MATLAB was used to produce all the figure that will be shown in the report.

## 4.1 Measuring time determination

The reason for determining the measuring time is to make sure that the time available at the Halde Haniel was used as efficiently as possible. However, it will be essential to have long enough measuring time to make sure that enough energy is emitted from the rock, so that the portable gamma-ray spectrometer can accurately determine the concentrations of the different elements. The measuring time was determined by measuring in the Green Village located on the campus of the TU Delft. There were two main criteria when selecting the different measuring locations. First, the location should consist of a flat surface. Secondly, the location should bare soil with a radius of half a meter, so no vegetation or buildings in the half a meter radius. In the Green Village, multiple buildings have been constructed. Also, the amount of vegetation has increased since the soil composition was determined. The two criteria taken into consideration, the following measuring locations have been selected (See figure 10).

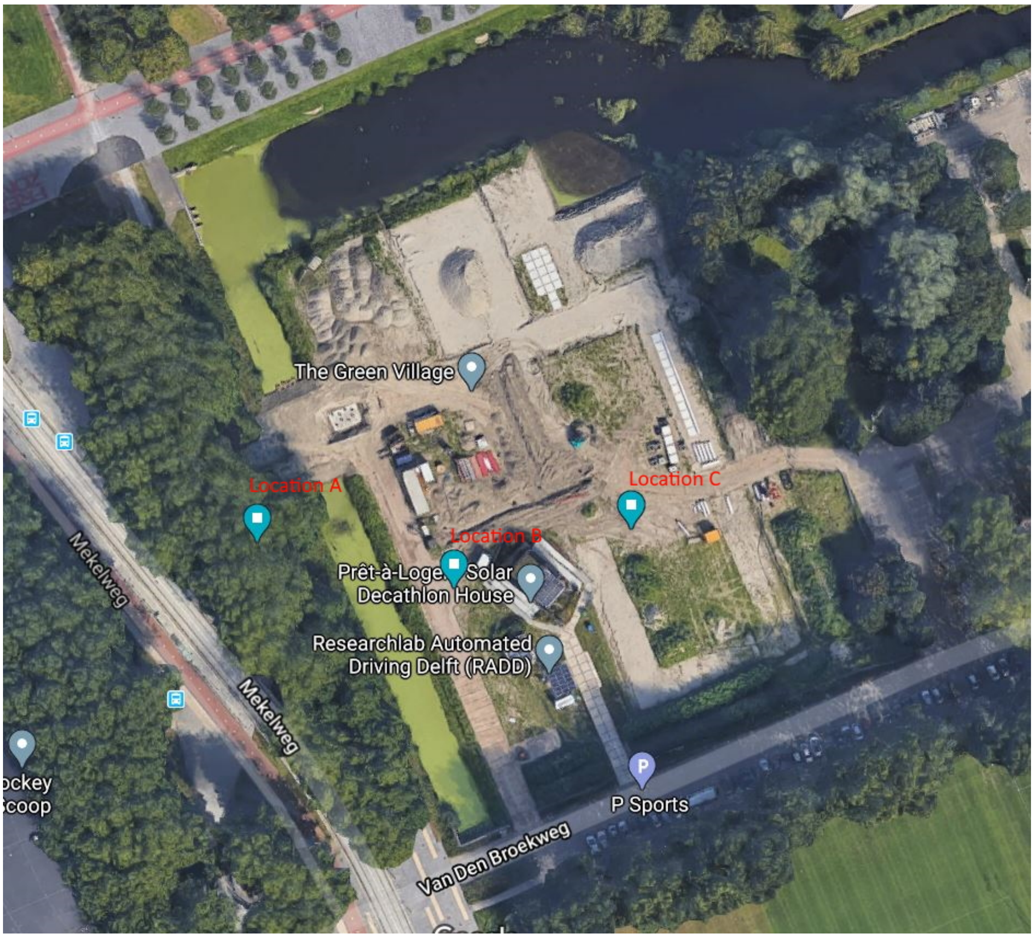


**Figure 10:** The measuring location in the Green Village (From Google Maps, 2020)

In figures A1, A2, A3, A3, A4 and A5, that are shown in appendix II, a visual representation of all measuring locations are shown. These figures are added to have a better idea of the weather and ground conditions on the measuring day. At every location there has been measured for 1, 2, 3, 4 and 6 minutes. The measurements were done on Monday 21 of February 2020 from 10:40 until 11:50. The temperature on that day was 7.5 degrees Celsius with an air humidity of 83 per cent. The water content in the soil has not been tested, but the 21 of February 2020 was a dry day. There was no visible water on the surface. However, the soil conditions were still very humid due to the rain that has fallen in days before the measurements.

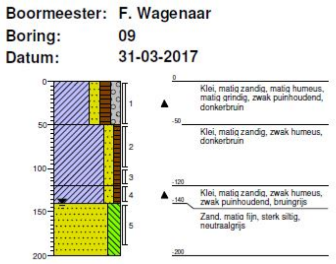


**(a)** Location A

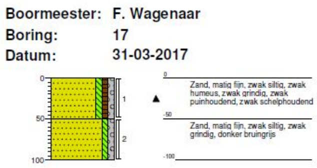


**(b)** Location B

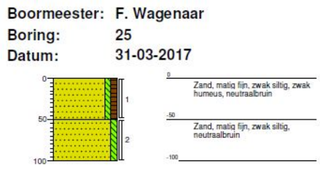


**(c)** Location C

**Figure 11:** Subsurface at the different locations

The soil information of the different locations is presented in figure 11, this information was provided by the Green Village. The soil information of the Green Village was used to determine three different locations with different soil types. However, due to all the buildings and vegetation present in the Green Village Location B and C show high similarity in the soil types and cannot be classified as different soil types. The coordinates of all three locations can be found in appendix II in table A2.

## 4.2 Locations of the in-field measurements at Halde Haniel

The field measurements were done at the spoil pile Halde Haniel, a facility of the active underground coal mine Prosper-Haniel near Bottrop, Germany (Doka, 2009). The measurements at the Halde Haniel were taken in 4 different ways, but all with the same measuring time. Furthermore, it was made sure that the measurements were done on a flat surface, but some measurements were done at the same angle as the sloped surface. The negative effects of vegetation on the measurements will be kept to a minimum. Therefore, all the measuring locations have been selected on having no vegetation in a radius of half a meter surrounding the measuring device. Since this location is open to the public, there were no limitations while doing the measurements. The coordinates of all the locations can be found the appendix III in table A4. In figure 12, an image of all the measuring locations in Google maps can be found. In the appendix III, figures A8 and A9 have been added as representation of two measuring locations. These figures are added to have a better idea of the weather and ground conditions on the measuring day.

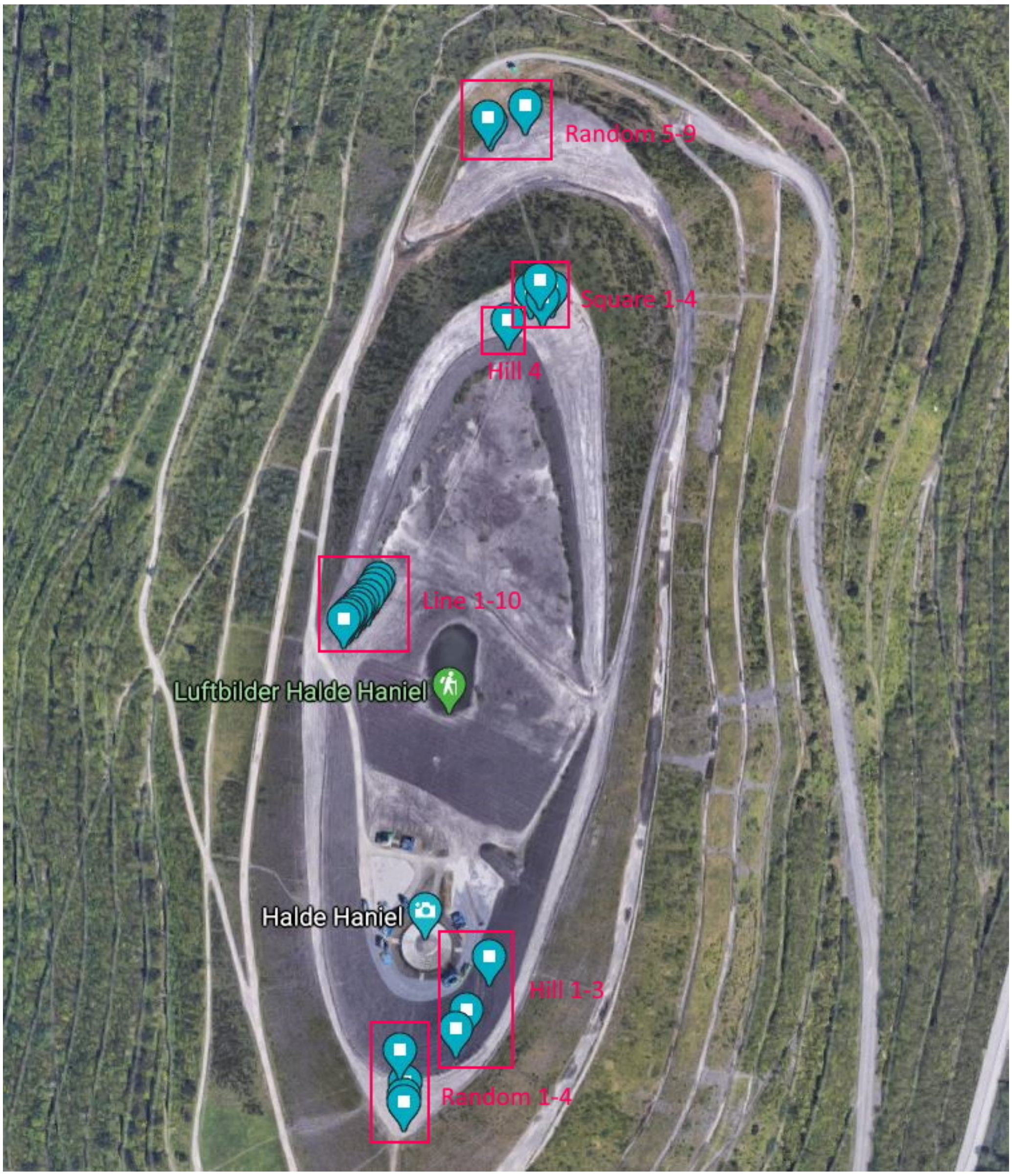


**Figure 12:** Locations at Halde Haniel (From Google Maps, 2020)

All measurements were done on the 3th of March 2020 from 10:15 until 13:45. On that day the temperature was 6 degrees Celsius with an air humidity of 77 per cent. The water content in the soil has not been tested, yet the 3th of March 2020 was a dry day. There was visible water on the surface. The water was a result of a significant amount of rain that fell in the days before the measurements.

There were taken in total nine 'random' measurements; these measurements were taken at different locations of the Halde Haniel site and could not be grouped with other measurements. In total, ten measurements were taken in a straight line with a spacing of approximately 3 meters. These measurements were tagged with the label 'Line' in the results. At the Halde Haniel site there are different slopes. On two different slope measurements were done. At every location on the slopes, three measurements with a spacing of one meter in the horizontal surface were taken. The first three measurements were taken with a vertical difference between them, and the fourth measurement was taken at a different location at the Halde Haniel site. These measurements were tagged with the label 'Hill' in the results. The last measuring location was creating a square with four measurements. These measurements were taken with a spacing of ten meters. The four measurements were tagged with the label 'square' in the results.

# 5 Results

## 5.1 Measuring time determination

Before starting with the measurements at the Halde Haniel site, some measurements were done in Delft. These measurements had as objective to have reliable measurements with a small error. Therefore, a measuring time for the Halde Haniel waste pile will be chosen, that suits both high & low radioactive rocks, the specific rock types for the region and will result in efficient fieldwork. The measurements were done on two different soil types. The results will give a difference between location A, and location B & C. Location A consists of clay with tree roots and location B & C of sand with some silt. Therefore the radiation at location A will be higher compared to location B & C. The results of these measurements are presented in the following paragraph.

In figure 13, the results of the measurements, at three different locations in Green Village situated in Delft, are shown including the error of the measurements. In table A3, the data from the three measurements in Delft are shown.

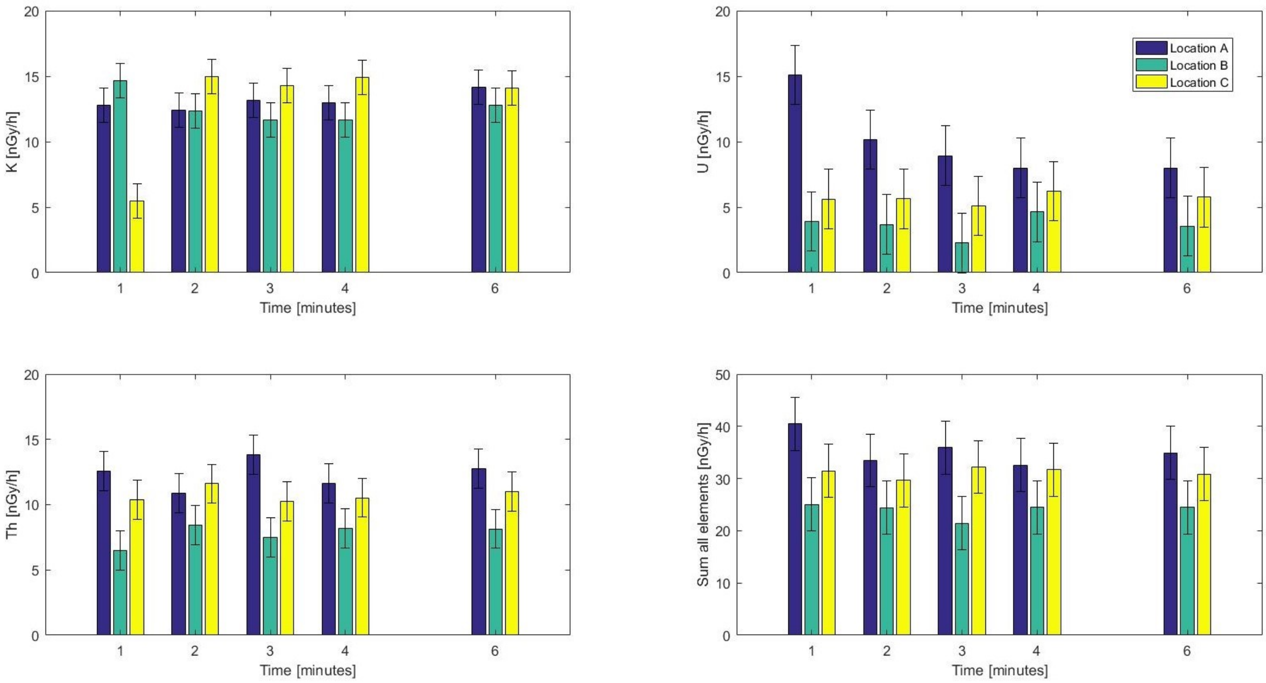


**Figure 13:** The data and error from the three different measuring locations in the Green Village in Delft are plotted. The vertical axis varies for each plot (K, U, Th and the sum of all the elements) and the horizontal axis displays the different measuring times

The error of the measurements affect the interpretation of the results a lot. The different measuring times have not resulted in data that is outside the measuring error. However, the exception is the one minute measurement. With a measuring time of one minute, the results are outside the error range of the other measurement. An example of this is the amount of Potassium (K) at location C (the top left bar graph). The one-minute measurement has a measured value around 5 nGy/h, while at 2, 3, 4 and 6 minutes, the measured value is around 15 nGy/h. The rest of the results are within the measuring error, only the Uranium concentration at location A is changing significantly over time (Top right bar plot). Here the amount of Uranium decreases over time, but is not stable at six minutes. From the measurements in Delft, a measuring time of one minute will not give accurate results. Therefore, a measuring time of one minute will not be used.

The spectrum graphs are analyzed to take a closer look at the measurements and their variations in time. In figure 14, the spectrum graph measured at location A & B in the Green Village for Potassium (K) is shown. The spectrum graph shows all the different channels that are used to determine the concentration of Potassium. There can be seen that a longer measuring time will result in more reported counts at both locations. A clear peak can be seen around channel 233. However, looking at the spectrum graphs of Uranium & Thorium in appendix II in figure A6 & A7 no clear peaks are shown in these spectrum graphs. For Potassium, a longer measuring time will result in more counts, but for Uranium and Thorium, this is not the case. With this information, the conclusion can be made that a longer measuring time will only result for an increasing amount of counts for Potassium (K), this will not be the case for Uranium (U) or Thorium (Th). The spectrum graphs suggest that there will be a difference in the amount of radiation depending on the measuring time. However, the final data per measurement is given in nano Gray per hour. Therefore, all the measurements are equalized for one hour. These equalized results are shown in figure 13. Figure 13 shows no significant difference for the varying measuring times, which could be concluded from spectrum graph (see figure 14).

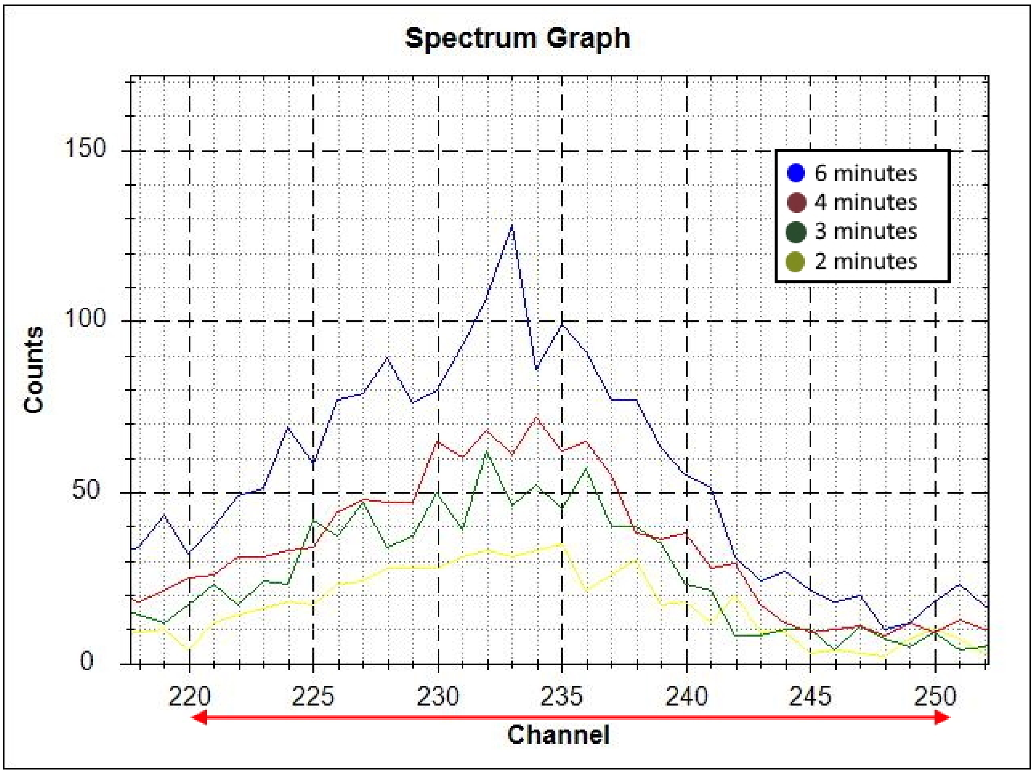


**(a)** Location A

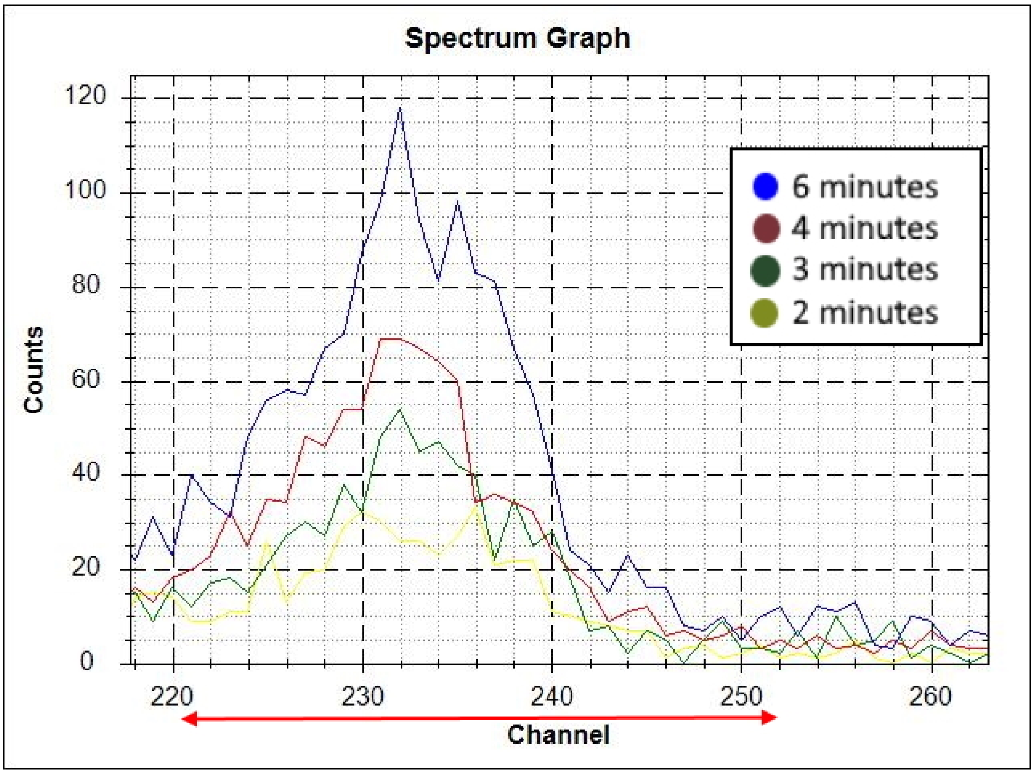


**(b)** Location B

**Figure 14:** The spectrum graph of location A & B. Where the red arrow indicates the range of channels that are used to determine the Potassium (K) concentration. On the horizontal axis and on the vertical axis the amount of counts per channel

The field measurements and the interpretation of the data were a good start for the determination of the measuring time. However, the field measurements did not give a conclusive answer. Therefore literature support will be needed. A sampling time of 2 min for highly radioactive rocks and 6 min for low radioactivity rocks is a reasonable compromise (IAEA, 2003). Besides IAEA (2003), the literature research for this study different measuring times for specific rocks types have been found. At the

Halde Haniel waste pile, the composition and the level of radiation is not known, but this information can be used to determine a correct measuring time. A measuring time of two minutes will be suitable for high radioactive rocks such as shales (but not for sandstones). A measuring time of four minutes will be suitable for shales and sandstones. The measuring time for limestones should be around ten minutes.

When the literature, the measurements that were done in the Green Village, and the criteria for Halde Haniel waste pile are considered, then there can be concluded that a measuring time of 4 minutes will be the most suitable in this study.

## 5.2 In-field measurements at Halde Haniel

In the ternary plot, shown in figure 15, the measurements at the Halde Haniel are clustered together. The shale and sandstone from the literature are very comparable to the data from the Halde Haniel. For the coal data, the amount of K and Th is not comparable to the measurements at the Halde Haniel. The significant difference between coal and the measurements makes sense, because the shale and sandstone are the waste product and the coal the valuable material.

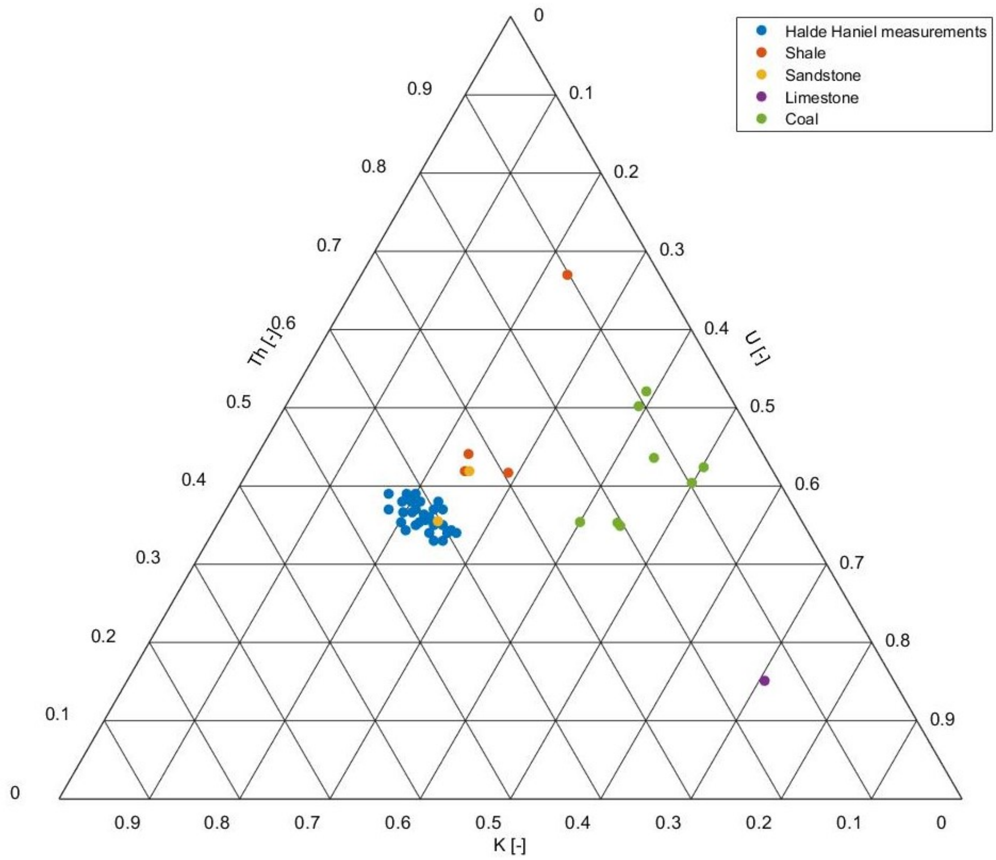


**Figure 15:** Ternary plot with the normalised data of K, U and Th retrieved from field measurements and literature to compare the overall difference in gamma radiation

When looking at figure 15 and figure 16, the two groups are still very clear. The first group of data points consists of the Halde Haniel data, shale and sandstone. The other group of data points consists of coal and limestone. The data for shale, sandstone and limestone are measured in England, but from the same geological period. Geological formations can vary a lot over such distance. However, data from the same geological formation will show more similarities than a geological formation from a different continent and geological period. For the literature data from coal, no measurements were available from Germany or Europe, so more data from literature was collected to compare better the overall amount of gamma radiation emitted from coal.

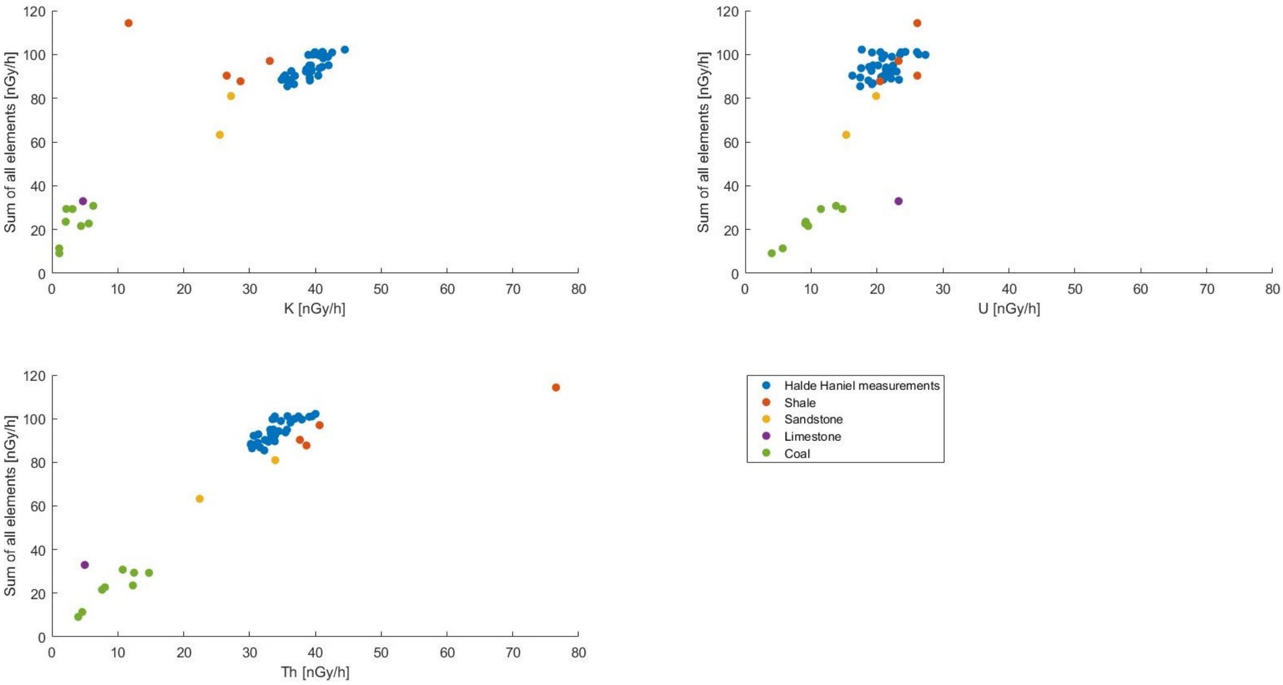


**Figure 16:** Total radiation of K (top-left), U (top-right) and Th (bottom-left) for the Halde Haniel (HH) measurements compared with the data retrieved from literature

In figure 17, a more zoomed-in plot of all the different measuring locations is shown, which reveals more detail from the data. One of the most exciting parts is that all the different measuring techniques are clustered together. Looking at the amount of Potassium (K) for the random measuring locations, every measuring location emits around 35 nGy/h (expect the two outliers). The clustering of data points is the same for the square measuring location and the line measuring location with an average emitted amount of radiation of 36.5 nGy/h and 39.5 nGy/h. This close range in K can not be seen in the slope measuring locations. This pattern is again shown in the amount of Thorium, but less precise than with the Potassium. When looking at the amount of Uranium (U), no pattern in the data can be determined. The amount of U is varying a lot in throughout the different measurements.

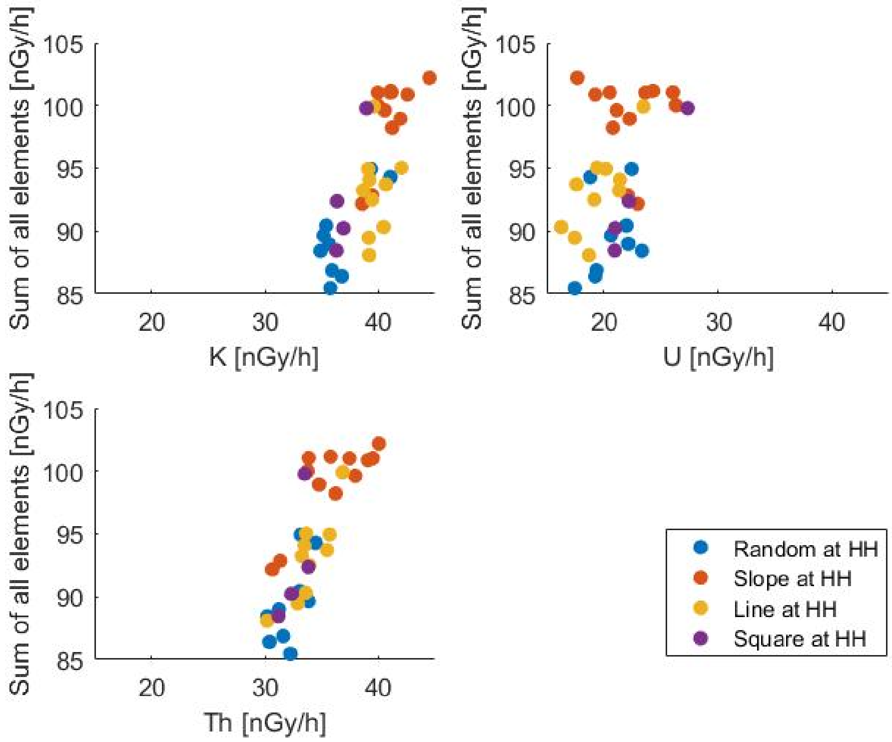


**Figure 17:** Zoom in of the Halde Haniel (HH) measurements to see the difference between the measuring sites. K (top-left), U (top-right) and Th (bottom-left)

All the measurements on the hills are very similar to each other except for two outliers. These outliers have two different reasons. Looking at table A5, the two outliers are H11 and H41. The reason that H11 is an outlier is that this was the first measurement on a slope. Therefore the placement of H11 was not perfect. During the measurement of H41 the receiver has fallen over, but this was for a short period of 2-6 seconds. An interesting remark to make the measuring location of the hill measurements 1,2 and 3 were around 400 metres away from hill measurement 4, but all locations gave results in the same range. When looking at the measurements taken on the horizontal surface of Halde Haniel waste pile (this includes the random, line and square measurements), no significant differences between the measuring locations were found, except that two outliers were present. The season for these outliers could not be determined due to the lack of information retrieved from the field. The random measurements were taken at two different places with a separation of approximately 500 metres. However, the results from these measurements are again very comparable to each other.

### 5.3 Hazard for humans

The information in table A5 will be used to see what the hazards for people will be. The average amount of radiation from all the measurements that were done at the waste pile Halde Haniel is 94.19 nGy/h, which is the absorbed gamma dose rate (D). To calculate the excess lifetime cancer risk equations (1) and (2) will be used. First equation (1) is used to calculate the annual effective dose rate (E).

$$E = 94.19 * 10^{-3} * 1.23 = 0.1159 mSv year^{-1} \tag{1}$$

To calculate the excess lifetime cancer risk equation (2) will be used. With average lifetime (ALT) for German people is around 80 years, the risk factor (RF) based on the fatal cancer risk is $0.5 * 10^{-4}$ and the annual effective dose rate (E) from equation (1).

$$ELCR = 0.1159 * 80 * 0.5 * 10^{-4} = 4.634 * 10^{-4} Sv^{-1} \tag{2}$$

# 6 Discussion

## 6.1 Time determination

From the results of the time determination, the moment that the longer measuring time would be redundant can easily be determined. The changes in results from 2, 3, 4 and 6 minutes were minimal, while a measuring time of 1 minute gave varying results. These variations are clearly shown in figure 13. When looking at Location A the amount of Uranium at one minute is 1.5 times larger than for the other measuring times. For the amount of Potassium at location C, the value measured at one minute is half the amount measured at the other locations. Furthermore, the information found in the literature was comparable to the field measurements results. Therefore, the measuring time of four minutes is sufficiently proven to be the standard in future research.

## 6.2 Field data versus literature data

The significant differences between the field measurements and some literature values is one of the most notable outcomes. From figure 16, there can be seen that both coal and limestone do not result in high amounts of gamma radiation. However, the radiation from shale and sandstone is very comparable to measurements done at the Halde Haniel waste pile. Since the values from the literature for some rocks are comparable to the field measurements, follow-up research will have to be conducted to determine the base values of the different rocks types. The base value measurements should be tested in the same way as the field measurements were done in this study. When these base measurements are done, the values can be used to make better conclusions on the content of the waste pile Halde Haniel.

## 6.3 Effects of weathering

Since the depth range of the portable gamma-ray spectrometer is 15 centimetres, merely the surface of the waste dump were measured. The top surface has been impacted the most to different weather conditions, such as wind, sunlight, rain and snow. Weathering modifies the concentration and distribution of the radioelements relative to that of fresh bedrock (IAEA, 2003). Since the waste pile Halde Haniel does not consist of fresh bedrock, the weathering effects can have a significant impact on the measurements. Measurements were done on the slopes of the Halde Haniel waste pile, so that the effects of weathering were reduced. The rocks on these slopes are less exposed to the weather conditions, than the rocks on the flat surfaces. However, the effect of gravitational erosion is higher on the slopes of the Halde Haniel waste pile. Therefore measuring on the slopes of the Halde Haniel waste pile will give a good indication on what the original emitted amounts of radiation are. To completely exclude the effects of weather conditions on the measurements, digging into the field area should be considered. The measurements done after digging into the field area could reveal a difference in the amount of gamma radiation emitted. The measurements done a greater depth will give results that are more comparable to the original amount of radiation present.

## 6.4 Soil Moisture

All the field measurements were done on the same day, which makes the data from this day comparable. However, for this reason, the effects of different weather and soil conditions (dry or wet) could not be determined. In literature, it is shown that soil moisture will have a significant impact on the measurements. However, nothing is mentioned about other factors that could influence the soil moisture (such as the porosity or compaction) (IAEA, 2003). Therefore, in future research, the impact of different weather and soil conditions should be monitored in greater detail. In the literature, the effect ten % of soil moisture will give an accuracy error of approximately ten % (IAEA, 2003), so the effects on the accuracy of the measurements could become very significant. Unfortunately, during the measuring day at the Halde Haniel waste pile, no soil samples were taken to determine the soil moisture. The soil moisture could be roughly determined with a visual reference of the measuring location (for example, a photo at every location). Unfortunately, the amount of photos taken in the field was low. Due to the lack of information about the soil moisture, the accuracy of the measurements can not be determined sufficiently. So this causes a significant issue to prove the reliability of all the measurements done during the fieldwork. In future research, the accuracy of the portable gamma-ray spectrometer should be tested to make sure that the measurements will have a high reliability.

Since the soil moisture has not been measured, the numbers in table 1 are an estimation of the real values. These errors could be used to reevaluate the results. However, with a measurement error of 50 per cent, the amount of radiation per year will stay below the maximum.

| **Amount of soil moisture [percent]** | **Maximum value** $[Sv^{-1}]$ | **Minimum value** $[Sv^{-1}]$ |
|---|---|---|
| no error | 0.000463 | 0.000463 |
| 10 | 0.000509 | 0.000417 |
| 20 | 0.000556 | 0.000370 |
| 50 | 0.000695 | 0.000231 |

**Table 1:** The range of the average amount of radiation per year with different soil moisture percentages

## 6.5 Hazard for humans

The level of radiation measured at the Halde Haniel waste pile is doubled than the measured levels in Delft. The excess lifetime cancer risk is eighty times smaller than the maximum value state by UNSCEAR (2000). So, the radiation coming from the waste pile Halde Haniel will give no health risk when staying there every day of the year. Since the Halde Haniel waste pile currently serves as a public park, the radiation will hardly affect the visitors of the park since the visiting time is short. However, the houses surrounding this area could have a higher risk on exposure to similar amounts of radiation or increased amounts of radiation, which could result in higher health risks for the inhabitants living in the area surrounding the Halde Haniel waste dump. Since two centimetres of vegetation cover can reduce the amount of radiation by 35 per cent (IAEA, 2003), this could be an option to reduce the chance on health risks for the people living next to the waste pile Halde Haniel.

## 6.6 The future of measuring technique

The full effects of soil moisture should be determined in a follow-up study. A change in soil moisture content can be very significant on the measuring error. Therefore, a follow-up study will be crucial for the determination of the accuracy of this technique. Not only the effects of soil moisture content should be measured, but also the effects of in-situ porosity and the compaction of the soil should be taken into account.

When the error of the measurements is determined, and the error of the measurement is reasonable, then a follow-up study could be done to develop a cheap and easy method without needing any large equipment for finding possible leftover resources in the waste piles. Furthermore, when determining the possible leftover resources in a waste pile, such as Halde Haniel, the different amount of radiations of the pure rocks should be tested to be able to determine the value of the waste that is left behind. These measurements should be done in combination with the determination of the local lithology. Also, if possible, the chemical composition of the rocks should be determined. If the results of the measurement error and the comparability of the pure rocks to mixed rock are promising, then waste piles can be re-processed, lowering the impact of mining on the environment.

# 7 Conclusion

Is the radiation at the waste dump Halde Haniel, a hazard for humans? This question can quickly be answered from the results of the measurements. In the results, it is already shown that values of the Halde Haniel are two times higher, compared to the measuring locations in Delft. The increase of these values may suggest a higher amount of gamma radiation in the Halde Haniel waste pile, which means that there will be a higher chance of health risks for humans in that area. However, the radiation measured on the Halde Haniel waste pile is eighty times smaller then the maximum stated by UNSCEAR (2000). Since, these results were produced without knowing the soil moisture. The measurement error due to the presence of soil moisture could give a large spread when producing the results again.

Measurements have been done at varying locations on the Halde Haniel waste dump with similar results. The variation measured in intensity is relatively consistent throughout the different measuring locations. However, when looking at the three different chemical elements, the intensity range becomes more substantial. Also, when comparing the different measuring locations, there are some notable differences, this holds especially for the measurements done on the slopes of Halde Haniel waste pile when comparing these measurements to the other measuring locations. Even though the measurement error will be relatively large, the spatial difference in the waste pile Halde Haniel will be more significant than this measuring error. In conclusion, spatial differences are noted in the Halde Haniel waste dump. Nevertheless, these differences could become even more significant when deeper measurements in the waste pile Halde Haniel are taken.

Since no soil samples have been taken during measuring day at the Halde Haniel, the environmental effects on the measurements can not be determined. Since soil moisture has a significant effect on the measurements and no tests were conducted to determine the amount of soil moisture at the different locations, there is no possibility to determine the accuracy of the portable gamma-ray spectrometer and the measurements done with this device.

To conclude, a portable gamma-ray spectrometer can be used to determine the amount of radiation that is emitted from a sample that consists of multiple rock types. However, to know the accuracy of these measurements, the soil moisture on the measuring location should be determined. When the soil moisture is not determined during the measurements, the chance of significant measurement errors will be increased. A significant measurement error will lead to unreliable measurements, which will provide problems when the data from this research will be compared to other studies.

## References


Beck, H. L. (1989). Radiation exposures due to fossil fuel combustion. *International Journal of Radiation Applications and Instrumentation. Part C. Radiation Physics and Chemistry*, *34*(2), 285–293. https://doi.org/10.1016/1359-0197(89)90236-1

Bem, H., Wieczorkowski, P., & Budzanowski, M. (2002). Evaluation of technologically enhanced natural radiation near the coal-fired power plants in the lodz region of poland. *Journal of Environmental Radioactivity*, *61*(2), 191–201. https://doi.org/10.1016/s0265-931x(01)00126-6

David G. Coles, R. C. R., & Ondov, J. M. (1979). Behavior of natural radionuclides in western coal fired power plants. *American Chemical Society*.

Doka, G. (2009). Life cycle inventory of the disposal of lignite spoil, coal spoil and coal tailings. *Doka Life Cycle Assessments*.

Fardy, J. J., Mcorist, G. D., & Farrar, Y. J. (1989). Neutron activation analysis and radioactivity measurements of australian coals and fly ashes. *Journal of Radioanalytical and Nuclear Chemistry Articles*, *133*(2), 217–226. https://doi.org/10.1007/bf02060494

Frank, O. (2009). Aspects of surface and environment protection in german mining areas. *Mining Science and Technology (China)*, *19*(5), 615–619. https://doi.org/10.1016/s1674-5264(09)60114-9

Gawor, Ł., Jankowski, A., & Ruman, M. (2011). Post-mining dumping grounds as geotourist attractions in the upper silesian coal basin and the ruhr district. *Moravian Geographical Reports*, *19*, 61–68.

Habib, M. A., Basuki, T., Miyashita, S., Bekelesi, W., Nakashima, S., Techato, K., Khan, R., Majlis, A. B. K., & Phoungthong, K. (2018). Assessment of natural radioactivity in coals and coal combustion residues from a coal-based thermoelectric plant in bangladesh: Implications for radiological health hazards. *Environmental Monitoring and Assessment*, *191*(1). https://doi.org/10.1007/s10661-018-7160-y

Harnischmacher, S. (2007). Anthropogenic impacts in the ruhr district (germany): A contribution to anthropogeomorphology in a former mining region, *30*, 185–192.

Harnischmacher, S. (2010). Quantification of mining subsidence in the ruhr district (germany). *Géomorphologie : relief, processus, environnement*, *16*(3), 261–274. https://doi.org/10.4000/geomorphologie.7965

Harris, C. D. (1946). The ruhr coal-mining district. *Geographical Review*, *36*(2), 194–221. https://doi.org/10.2307/210876

Hellman, S. (2020). https://www.halden.ruhr/halde-haniel.html

IAEA. (2003). Guidelines for radioelement mapping using gamma ray spectrometry data.

IRCP, ( C. o. R. P. (1990). Recommendations of the international commission on radiological protection. *Oxford: UK Pergamon Press*.

ISU. (2006). The international system of units (si), 8th edition. *Chemistry International – Newsmagazine for IUPAC*, *28*(5). https://doi.org/10.1515/ci.2006.28.5.30a

Knoll, G. F. (2012). *Radiation detection and measurement*. John Wiley & Sons.

Kolo, M., Amin, Y., Khandaker, M., & Abdullah, W. (2017). Radionuclide concentrations and excess lifetime cancer risk due to gamma radioactivity in tailing enriched soil around maiganga coal mine, northeast nigeria. *International Journal of Radiation Research*, *15*(1), 71–80. https://pdfs.semanticscholar.org/ba5b/93125b3c0c5dfd0220a1045bd543febc7504.pdf

Koomans. (2000). *Sand in motion: Effects of density and grain size* (Doctoral dissertation). University of Groningen.

Løvborg, L. (1984). *The calibration of portable and airborne gamma-ray spectrometers - theory, problems, and facilities*. Danmarks Tekniske Universitet, Risø Nationallaboratoriet for Bæredygtig Energi.

Myers, K. J. (1987). Onshore outcrop gamma ray spectrometry as a tool in sedimentological studies.

Njinga, R. L., & Tshivhase, V. M. (2016). Lifetime cancer risk due to gamma radioactivity in soils from tudor shaft mine environs, south africa. *Journal of Radiation Research and Applied Sciences*, 310–315. https://doi.org/10.1016/j.jrras.2016.02.003

Nordrhein-Westfalen, G. D. (2015). Die erdgeschichte unseres landes. https://www.gd.nrw.de/ge_ev_stratigraphie.htm

Parkinson, D. N. (1996). Gamma-ray spectrometry as a tool for stratigraphical interpretation: Examples from the western european lower jurassic. *Sequence Stratigraphy in British Geology, Geological Society Special Publication*, *103*, 231–255.

SatisGeo. (2020). Instruments for geophysics and environment. https://satisgeo.com/

Tracy, B., & Prantl, F. (1985). Radiological impact of coal-fired power generation. *Journal of Environmental Radioactivity*, *2*(2), 145–160. https://doi.org/10.1016/0265-931x(85)90004-9

UNSCEAR. (2000). Sources and effects of ionizing radiation, united nations scientific committee on the effects of atomic radiation (unscear) 2000 report, volume i. *United Nations Scientific Committee on the Effects of Atomic Radiation (UNSCEAR) Reports*. https://doi.org/10.18356/49c437f9-en

# I Appendix

| **Geological period** | **Rock type** | **K [nGy/h]** | | **Th [nGy/h]** | | **U [nGy/h]** | | **Sum** | | **Reference** | **Region** |
|---|---|---|---|---|---|---|---|---|---|---|---|
| | | Mean | std | Mean | std | Mean | std | mean | std | | |
| Devonian | Siltstones | 11.64 | 4.45 | 76.57 | 20.45 | 26.11 | 7.95 | 114.31 | 32.84 | | |
| Devonian | Grey shale | 33.09 | 3.27 | 40.65 | 3.24 | 23.27 | 3.06 | 97.01 | 9.58 | | |
| Devonian | Mudstones | 28.64 | 3.27 | 38.66 | 3.74 | 20.43 | 2.78 | 87.73 | 9.79 | | |
| Carboniferous | Grey shales/Siltstones | 26.55 | 2.09 | 37.66 | 2.99 | 26.11 | 3.97 | 90.31 | 9.06 | (Myers, 1987) | England |
| Carboniferous | Fine Grained Sandstones | 27.20 | 3.14 | 33.92 | 6.73 | 19.86 | 3.97 | 80.98 | 13.85 | | |
| Carboniferous | Medium Grained Sandstone | 25.50 | 3.79 | 22.45 | 4.24 | 15.32 | 7.38 | 63.27 | 15.41 | | |
| Carboniferous | Limestone | 4.71 | 5.23 | 4.99 | 4.74 | 23.27 | 7.95 | 32.96 | 17.91 | | |
| | Coal | 1.12 | 0.22 | 3.99 | 0.80 | 4.03 | 0.81 | 9.14 | 1.83 | (David G. Coles and Ondov, 1979) | USA |
| | Coal | 2.17 | 0.43 | 12.47 | 2.49 | 14.76 | 2.95 | 29.40 | 5.88 | | |
| | Coal | 5.59 | 0.43 | 8.05 | 0.48 | 9.10 | 0.90 | 22.73 | 1.81 | | |
| | Coal | 4.42 | 1.05 | 7.62 | 1.15 | 9.56 | 1.45 | 21.60 | 3.64 | (Bem et al., 2002) | Poland |
| | Coal | 6.27 | 0.75 | 10.75 | 0.95 | 13.79 | 2.16 | 30.81 | 3.86 | | |
| | Coal | 1.10 | 0.03 | 4.61 | 0.18 | 5.70 | 0.14 | 11.41 | 0.35 | (Tracy and Prantl, 1985) | Canada |
| | Coal | 3.13 | 1.22 | 14.74 | 1.84 | 11.49 | 4.37 | 29.36 | 7.43 | (Fardy et al., 1989) | Australia |
| | Coal | 2.09 | 0.73 | 12.29 | 29.18 | 9.19 | 67.78 | 23.57 | 97.69 | (Beck, 1989) | USA |

**Table A1:** The information for specific rocks types with the mean value, standard deviation, geological period, the source and the region of the rocks

# II Appendix (Delft)

## Time determination Delft

### Methods

| | Longitude | Latitude |
|---|---|---|
| **Location A** | **51.996268** | **4.376941** |
| **Location B** | **51.996167** | **4.377520** |
| **Location C** | **51.9962829** | **4.378085** |

**Table A2:** Coordinates of the three measuring locations in the Green Village

**Figure A1:** Location A

**Figure A2:** Location A

**Figure A3:** Location B

**Figure A4:** Location B

**Figure A5:** Location C

## Results

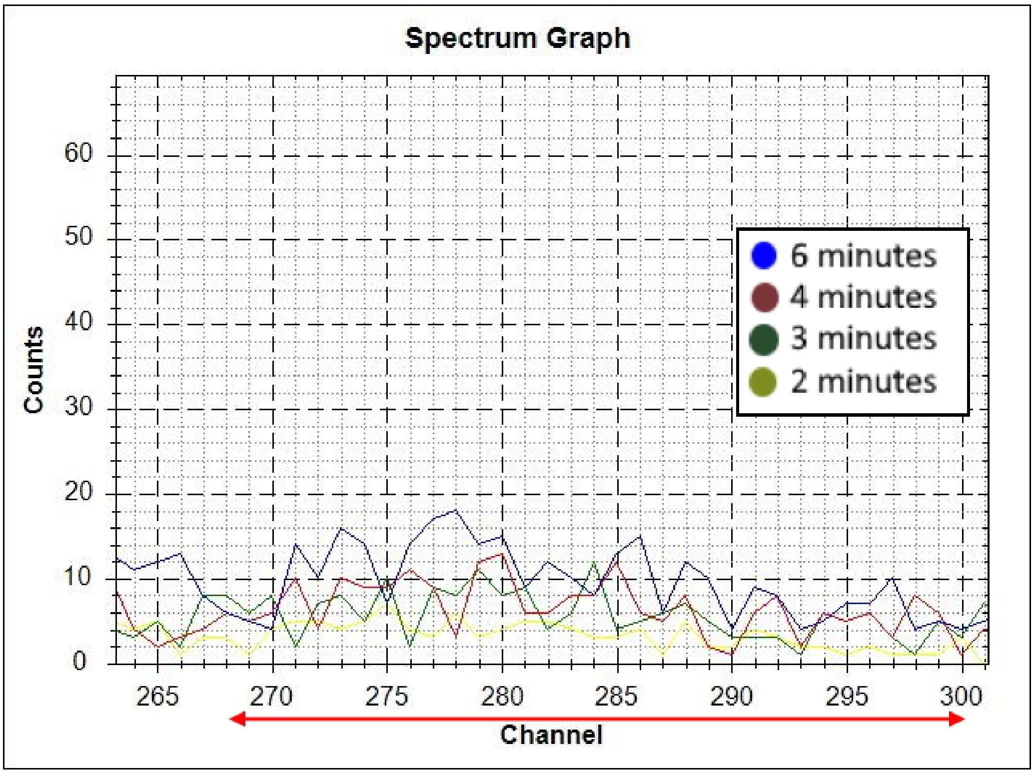


**(a)** Location A

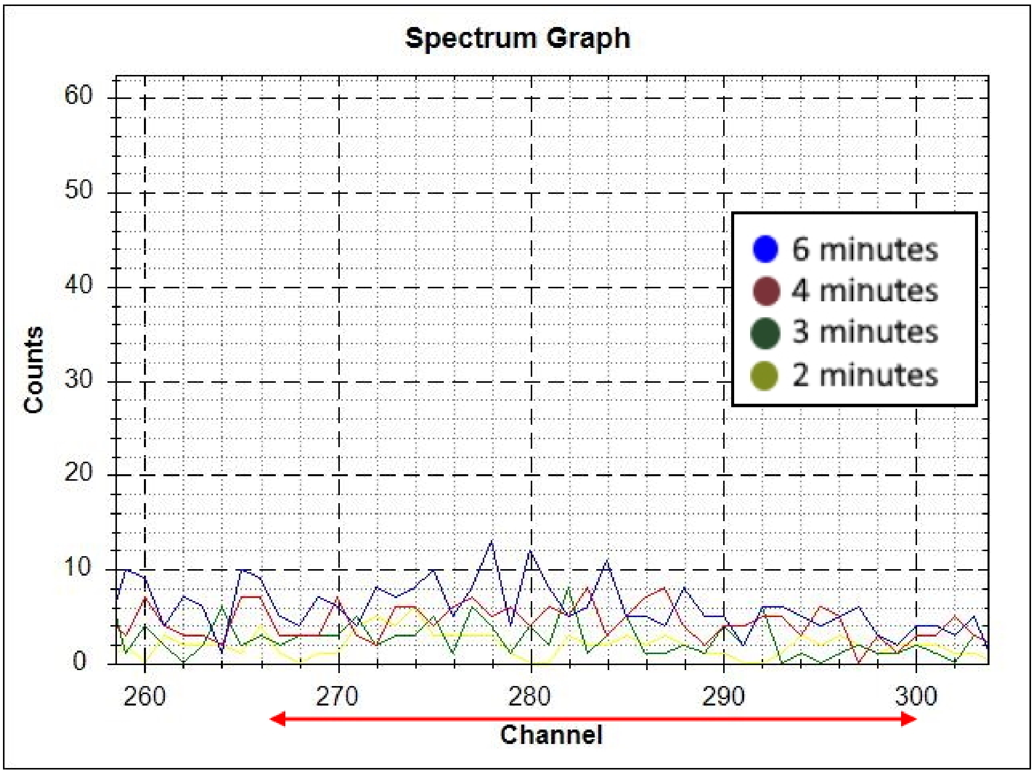


**(b)** Location B

**Figure A6:** The spectrum graph of location A & B. Where the red arrow indicates the range of channels that are used to determine the Uranium (U) concentration. On the horizontal axis and on the vertical axis the amount of counts per channel

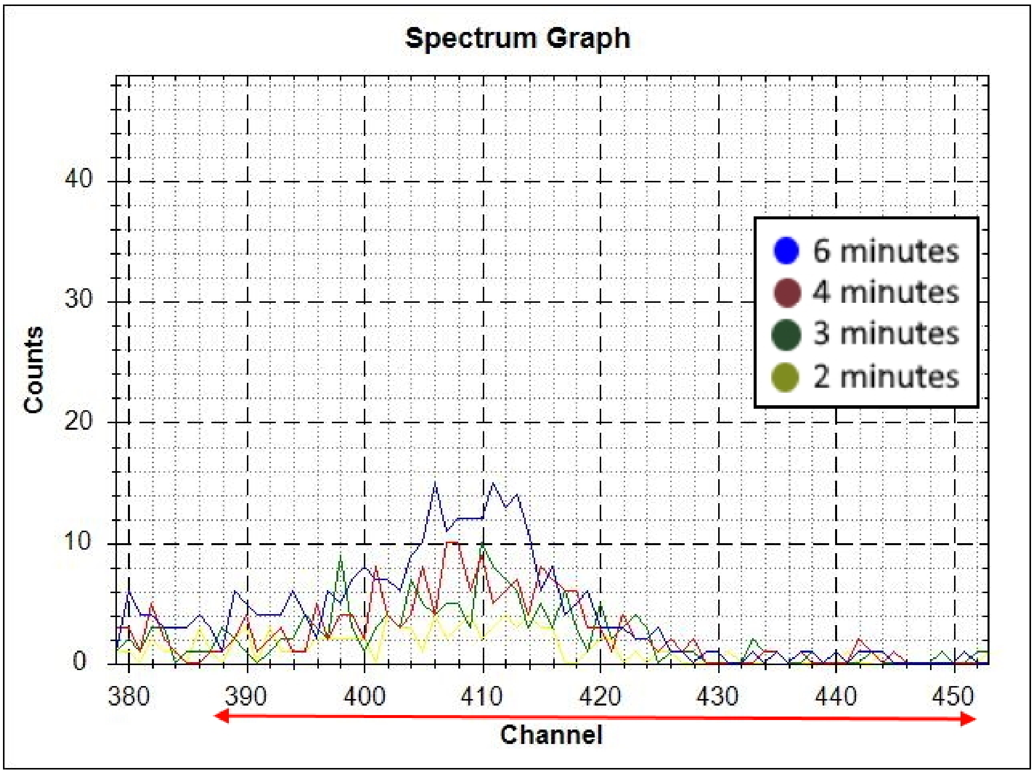


**(a)** Location A

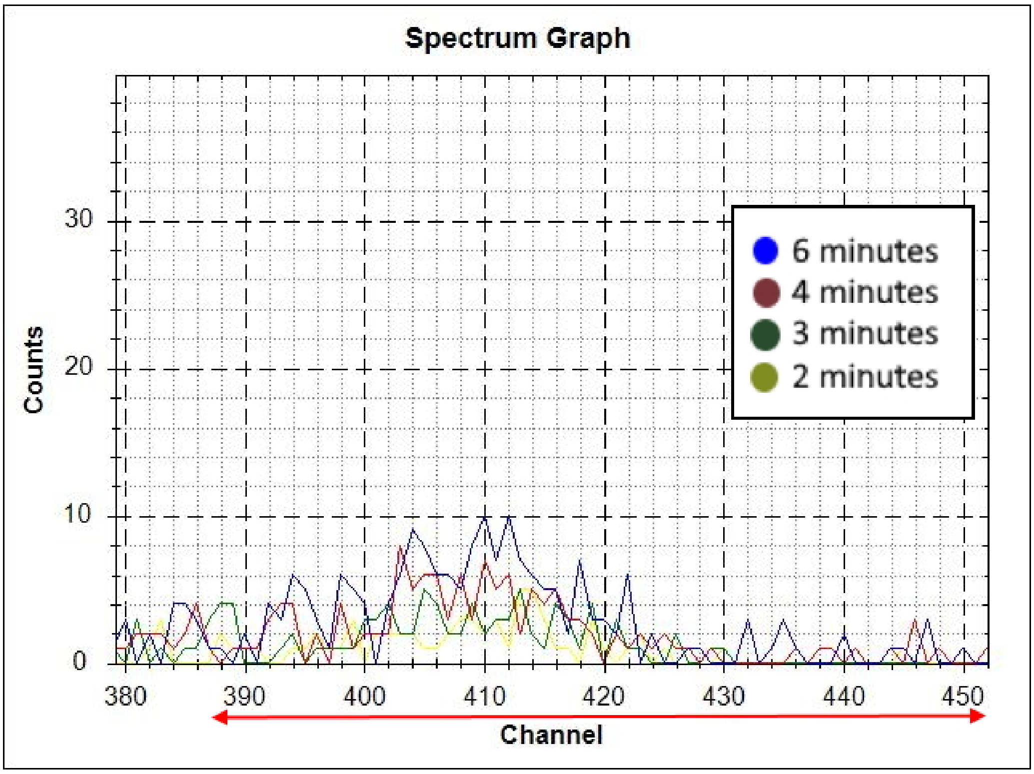


**(b)** Location B

**Figure A7:** The spectrum graph of location A & B. Where the red arrow indicates the range of channels that are used to determine the Thorium (Th) concentration. On the horizontal axis and on the vertical axis the amount of counts per channel

| **Place** | **K [nGy/h]** | **U [nGy/h]** | **Th [nGy/h]** | **SUM [nGy/h]** | **Date Time** | **Measurement Time** |
|---|---|---|---|---|---|---|
| A1 | 12.81 | 15.1 | 12.59 | 40.5 | 02/21/2020 10:56:46 | 00:01:00 |
| A2 | 12.42 | 10.16 | 10.88 | 33.46 | 02/21/2020 10:55:10 | 00:02:00 |
| A3 | 13.16 | 8.92 | 13.84 | 35.92 | 02/21/2020 10:52:16 | 00:03:00 |
| A4 | 12.96 | 7.99 | 11.61 | 32.57 | 02/21/2020 10:48:55 | 00:04:00 |
| A6 | 14.17 | 7.99 | 12.76 | 34.91 | 02/21/2020 10:44:09 | 00:06:00 |
| B1 | 14.65 | 3.91 | 6.49 | 24.46 | 02/21/2020 11:04:21 | 00:01:00 |
| B2 | 12.32 | 3.68 | 8.44 | 24.51 | 02/21/2020 11:06:43 | 00:02:00 |
| B3 | 11.64 | 2.27 | 7.51 | 21.42 | 02/21/2020 11:10:14 | 00:03:00 |
| B4 | 11.68 | 4.64 | 8.19 | 24.45 | 02/21/2020 11:14:35 | 00:04:00 |
| B6 | 12.76 | 3.55 | 8.15 | 25.04 | 02/21/2020 11:20:59 | 00:06:00 |
| C1 | 15.46 | 5.61 | 10.39 | 31.46 | 02/21/2020 11:40:17 | 00:01:00 |
| C2 | 14.31 | 5.1 | 10.25 | 29.66 | 02/21/2020 11:38:58 | 00:02:00 |
| C3 | 14.96 | 5.64 | 11.6 | 32.2 | 02/21/2020 11:36:19 | 00:03:00 |
| C4 | 14.92 | 6.23 | 10.53 | 31.69 | 02/21/2020 11:32:59 | 00:04:00 |
| C6 | 14.09 | 5.76 | 10.99 | 30.83 | 02/21/2020 11:28:38 | 00:06:00 |

**Table A3:** The measuring data from every measurement at the Green Village in Delft with the time specified, the amount of radiation from the different elements and the time and date when the measurement was done

# III Appendix (Halde Haniel)

## Halde Haniel

### methods

| | Longitude | Latitude |
|---|---|---|
| Random 1 | 51.549366 | 6.876295 |
| Random 2 | 51.549405 | 6.876300 |
| Random 3 | 51.549474 | 6.876307 |
| Random 4 | 51.549649 | 6.876260 |
| Slope 1 | 51.549760 | 6.876752 |
| Slope 2 | 51.549856 | 6.876851 |
| Slope 3 | 51.550138 | 6.877042 |
| Line 1 | 51.552001 | 6.875750 |
| Line 2 | 51.552016 | 6.875783 |
| Line 3 | 51.552034 | 6.875815 |
| Line 4 | 51.552058 | 6.875852 |
| Line 5 | 51.552079 | 6.875885 |
| Line 6 | 51.552101 | 6.875915 |
| Line 7 | 51.552126 | 6.875959 |
| Line 8 | 51.552161 | 6.875999 |
| Line 9 | 51.552190 | 6.876032 |
| Line 10 | 51.552218 | 6.876058 |
| Slope 4 | 51.553649 | 6.877211 |
| Square 1 | 51.553766 | 6.877521 |
| Square 2 | 51.553819 | 6.877602 |
| Square 3 | 51.553862 | 6.877496 |
| Square 4 | 51.553809 | 6.877413 |
| Random 5 | 51.554765 | 6.877058 |
| Random 6 | 51.554789 | 6.877023 |
| Random 7 | 51.554852 | 6.877363 |
| Random 8 | 51.554852 | 6.877363 |
| Random 9 | 51.554852 | 6.877363 |

**Table A4:** Coordinates of the measuring locations on the Halde Haniel waste pile

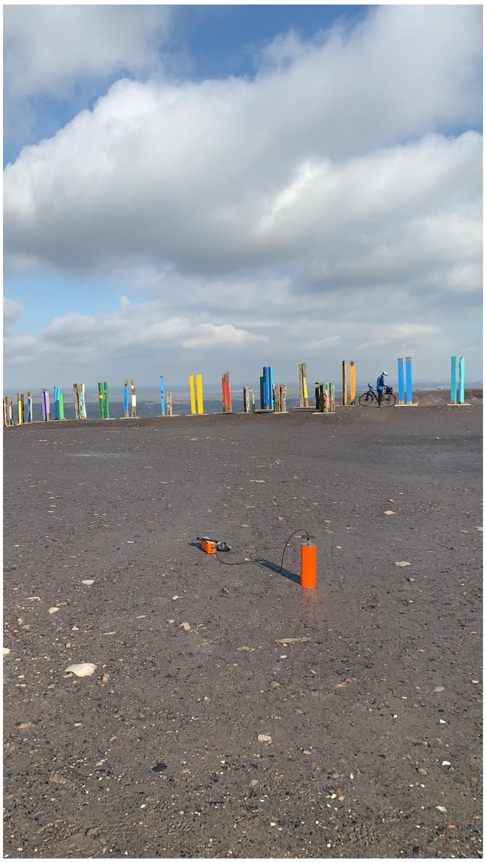

**Figure A8:** Location Halde Haniel

**Figure A9:** Location on slope at Halde Haniel

**Results**

| | K [nGy/h] | U [nGy/h] | Th [nGy/h] | SUM [nGy/h] | Date Time |
|---|---|---|---|---|---|
| **R1** | 35.91 | 19.35 | 31.61 | 86.87 | 03/03/2020 10:27:59 |
| **R2** | 35.76 | 17.45 | 32.25 | 85.46 | 03/03/2020 10:32:46 |
| **R3** | 34.89 | 23.33 | 30.22 | 88.44 | 03/03/2020 10:39:15 |
| **R4** | 35.17 | 20.63 | 33.85 | 89.65 | 03/03/2020 10:44:41 |
| **H11** | 38.57 | 22.97 | 30.64 | 92.18 | 03/03/2020 10:52:19 |
| **H12** | 42.56 | 19.24 | 39.08 | 100.88 | 03/03/2020 11:01:24 |
| **H13** | 39.94 | 23.64 | 37.45 | 101.03 | 03/03/2020 11:06:09 |
| **H21** | 41.2 | 20.79 | 36.23 | 98.23 | 03/03/2020 11:10:33 |
| **H22** | 39.94 | 26.32 | 33.76 | 100.02 | 03/03/2020 11:15:31 |
| **H23** | 41.08 | 24.3 | 35.78 | 101.16 | 03/03/2020 11:19:55 |
| **H31** | 40.55 | 21.12 | 37.96 | 99.63 | 03/03/2020 11:24:20 |
| **H32** | 41.14 | 26.06 | 33.85 | 101.05 | 03/03/2020 11:30:12 |
| **H33** | 41.93 | 22.25 | 34.77 | 98.95 | 03/03/2020 11:34:39 |
| **L1** | 39.6 | 23.47 | 36.85 | 99.92 | 03/03/2020 11:39:00 |
| **L2** | 39.09 | 20.17 | 35.7 | 94.96 | 03/03/2020 11:48:17 |
| **L3** | 42.02 | 19.4 | 33.62 | 95.05 | 03/03/2020 11:53:00 |
| **L4** | 39.2 | 21.4 | 33.48 | 94.09 | 03/03/2020 11:57:22 |
| **L5** | 40.46 | 16.26 | 33.6 | 90.32 | 03/03/2020 12:01:43 |
| **L6** | 39.14 | 17.45 | 32.88 | 89.47 | 03/03/2020 12:30:53 |
| **L7** | 39.44 | 19.15 | 33.91 | 92.51 | 03/03/2020 12:35:16 |
| **L8** | 40.65 | 17.6 | 35.47 | 93.72 | 03/03/2020 12:39:37 |
| **L9** | 39.18 | 18.7 | 30.21 | 88.09 | 03/03/2020 12:43:56 |
| **L10** | 38.66 | 21.33 | 33.25 | 93.24 | 03/03/2020 12:48:19 |
| **H41** | 39.45 | 22.07 | 31.35 | 92.86 | 03/03/2020 12:52:48 |
| **H42** | 44.49 | 17.68 | 40.04 | 102.2 | 03/03/2020 13:00:01 |
| **H43** | 41.02 | 20.52 | 39.5 | 101.04 | 03/03/2020 13:04:20 |
| **V1** | 38.94 | 27.35 | 33.5 | 99.79 | 03/03/2020 13:08:49 |
| **V2** | 36.36 | 22.2 | 33.82 | 92.38 | 03/03/2020 13:15:27 |
| **V3** | 36.31 | 20.95 | 31.2 | 88.46 | 03/03/2020 13:20:52 |
| **V4** | 36.91 | 20.98 | 32.34 | 90.23 | 03/03/2020 13:25:23 |
| **R5** | 35.4 | 21.98 | 33.06 | 90.44 | 03/03/2020 13:29:56 |
| **R6** | 39.36 | 22.43 | 33.16 | 94.95 | 03/03/2020 13:36:38 |
| **R7** | 41.04 | 18.81 | 34.46 | 94.3 | 03/03/2020 13:41:27 |
| **R8** | 35.62 | 22.14 | 31.24 | 88.99 | 03/03/2020 13:46:11 |
| **R9** | 36.76 | 19.24 | 30.4 | 86.41 | 03/03/2020 13:51:22 |

**Table A5:** The measuring data from every measurement on the Halde Haniel waste pile in Germany with the time specified, the amount of radiation from the different elements and the time and date when the measurement were done